

# SUTRA: A Novel Approach to Modelling Pandemics with Applications to COVID-19

Manindra Agrawal, Madhuri Kanitkar and M. Vidyasagar <sup>\*</sup>

February 28, 2025

## Abstract

In this paper, we present a new mathematical model for pandemics called SUTRA. The acronym stands for Susceptible, Undetected, Tested (positive), and Removed Approach. A novel feature of our model is that it allows estimation of parameters from reported infection data, unlike most other models that estimate parameter values from other considerations. This gives the model the ability to predict the future trajectory well, as long as parameters do not change. In addition, it is possible to quantify how the model parameter values were affected by various interventions to control the pandemic, and/or the arrival of new mutants.

We have applied our model to analyze and predict the progression of the COVID-19 pandemic in several countries. We present our predictions for two countries: India and US. In both cases, the model-computed trajectory closely matches actual one. Moreover, our predictions were used by entities such as the Reserve Bank of India to formulate policy.

## 1 Introduction

### 1.1 Background

The COVID-19 pandemic caused by the SARS-CoV-2 virus has by now led to more than 230 million reported cases and more than 4.7 million deaths worldwide [34]. By way of comparison, the influenza epidemic of 1957 led to 20,000 deaths in the UK and 80,000 deaths in the USA, while the 1968 influenza pandemic led to 30,000 deaths in the UK and 100,000 deaths in the USA [16]. In contrast, the COVID-19 pandemic has already led to more than 700,000 deaths in the USA and 135,000 deaths in the UK through multiple waves [34]. Even allowing for the increase in population during the past half-century, it is evident that the current pandemic is the most deadly since the “Spanish flu” of 1918–19, when an estimated 675,000 people died in the USA [6]. Among large economies, the USA, UK, Italy, and Spain, have all registered between 1,800 and 2,100 deaths per million population [34]. In these countries, the pandemic appeared to have abated, only to return with a second, third, or even a fourth wave [29, 34]. In the USA and the UK, during the first three waves, each wave was more severe than its predecessor, both in terms of the number of daily new cases and deaths. However, the fourth wave saw a significantly lower rate of hospitalizations and deaths. India had a relatively benign first wave, with just around one hundred deaths per million

---

<sup>\*</sup>MA is with the Department of Computer Science, Indian Institute of Technology Kanpur, Kanpur, UP 208016. MK is Deputy Chief Integrated Defence Staff (Medical), Headquarters Integrated Defence Staff, Ministry of Defence, New Delhi. MV is with the Department of Artificial Intelligence, Indian Institute of Technology Hyderabad. Corresponding author; Email: M.Vidyasagar@iith.ac.in

population. However, it went through a much more ferocious second wave that is essentially over now. Despite the second wave, India ranks at no. 120 with 320 deaths per million, and at no. 127 with 24,054 cases per million [34]. However, because of its large population, in absolute numbers India has registered the second largest number of cases after the USA, and the third highest number of deaths after the USA and Brazil [34].

In order to cope with a health crisis of this magnitude, governments everywhere would require accurate projections of the progress of the pandemic, both in space and over time. Over the past century or so, various epidemiological models have been developed, as reviewed in the next section. All of these models are based on the premise that the disease spreads when an infected person comes into contact with a susceptible person.

There are two major challenges in adopting such models for COVID-19. First, a large majority of cases remain undetected. Estimates for percentage of undetected cases are region-dependent: for US it is around 76% [5] while for India it is around 97% [27]. Undetected cases are the primary drivers of spread of infection since nearly all detected cases get quarantined. Second, the effective population over which the pandemic is active has changed significantly with time due to various control measures taken. This has been the primary reason for multiple peaks observed in various countries, as we demonstrate later. In order to correctly capture the trajectory of the pandemic, percentage of undetected cases as well as change in effective population with time needs to be estimated. This is not easy. The direct way to estimate number of undetected cases is to conduct regular serosurveys which is both expensive and difficult. To estimate effective population, one may count population of only those regions that have reported cases, however, this is likely to be an overestimate since many people in these regions may have completely isolated themselves taking them outside the reach of pandemic. Moreover, this will miss regions with all undetected cases completely.

## 1.2 Motivation

There is no shortage of mathematical models for the progression of a pandemic such as COVID-19. Indeed, dozens if not hundreds of models have been proposed during the past eighteen to twenty months. In many mathematical models, the emphasis is on traditional themes such as stability and convergence of the solution trajectories to equilibria or limit cycles. Many of the models are so elaborate that it would be impossible to identify all the parameters of the model from available data. Against this background, we were motivated by the following considerations:

- Our primary motivation was to make *verifiable predictions that would guide policy-makers*. Thus we aimed to predict *the number of daily new cases* reported in various states in India. These could in turn be translated, using prior experience, into the anticipated load on the healthcare system.
- Any modelling methodology that is applicable to a practical situation must take into account that *the parameters of the pandemic are not constant with time*. Rather, they change due to multiple factors including the inner dynamics of the pandemic and interventions to control its spread. To illustrate: when the Delta variant hit India with full force, starting in late February 2021, the fraction of Delta in the viral genome sequences isolated from patients went from 0% to about 85% in just three or four weeks [17]. This caused the contact rate of the pandemic to jump from 0.23 to 0.38 during the period. Also, nonpharmaceutical interventions such as lockdowns cause “jump” discontinuities in the contact rate.

Therefore the traditional asymptotic results of system identification theory, showing that estimates converge to their true values as time goes to infinity, are not of much utility.

- We were interested in a *systematic procedure* to determine when the parameters of the pandemic changed sufficiently that a recalibration was required. By its very nature, the identification of transition period will always be a little inexact. A corollary of the above statement is that we need a model whose predictions are accurate so long as the parameters don't change, *and we have a way to determine when they are changing*. This leads to the notion of "phases" in the course of the pandemic, whose duration is not fixed; it depends on when the parameter values change.

In short, our motivation was to provide a solution that worked. At the same time, it needed to be amenable to mathematical analysis so that parameter estimation from data is algorithmically feasible.

### 1.3 Our Contributions

We formulate a new mathematical model for the spatial and temporal evolution of a pandemic in the presence of significant undetected cases. The model includes a parameter to estimate the number of undetected cases and another parameter to estimate effective population. The biggest novelty of the model is that it admits a *numerically robust method for estimating the parameters in the model from the available data* as discussed in the motivation section. This has important consequences.

First, the model can predict the future course of the pandemic as long as the parameter values do not change significantly:

- In April this year, the Indian second wave was at its worst, with the cases and deaths mounting, seemingly without an end in sight. On April 29th we predicted [24] that (the seven-day moving average of) the cases would hit the peak between May 4th and 8th, and would peak at around 390K cases. At that time other models were predicting numbers from 800K to one million. In the event, the actual peak came on 8th May at 392K – a very good match. In fact, the actual trajectory remained very close to the predicted trajectory for next two months as can be seen in Figure 1.
- Another example is the prediction made by the model on 25th July for peak in US [23]. It indicated peak in August-end at around 152K infections per day. The actual peak arrived on 1st September at 166K infections per day (ignoring the one day jump to 172K on 13th September) (see Figure 2).
- Subsequently we made several predictions about a possible "third wave" in India, and came to the conclusion that it was unlikely, unless the Delta variant was replaced by a still more infectious variant. This prediction was taken seriously by many, including the Reserve Bank of India in its "State of the Economy" survey in mid-August 2021 [26].

Second major consequence of parameter estimation from data is that a post-facto analysis can be done of events causing significant change in trajectory of the pandemic in a region, and their impact can be quantified. For example, the efficacy of a lockdown, or the change in spread rate due to a new variant, or expansion of pandemic to new regions. Later in the paper, we do such an analysis for India and US.

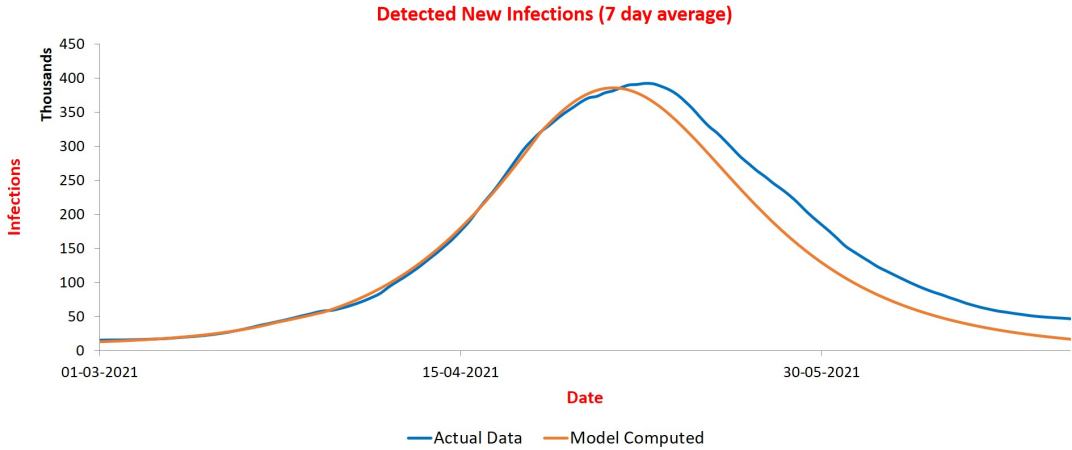


Figure 1: Predicted India Trajectory on 29th April 2021 versus actual

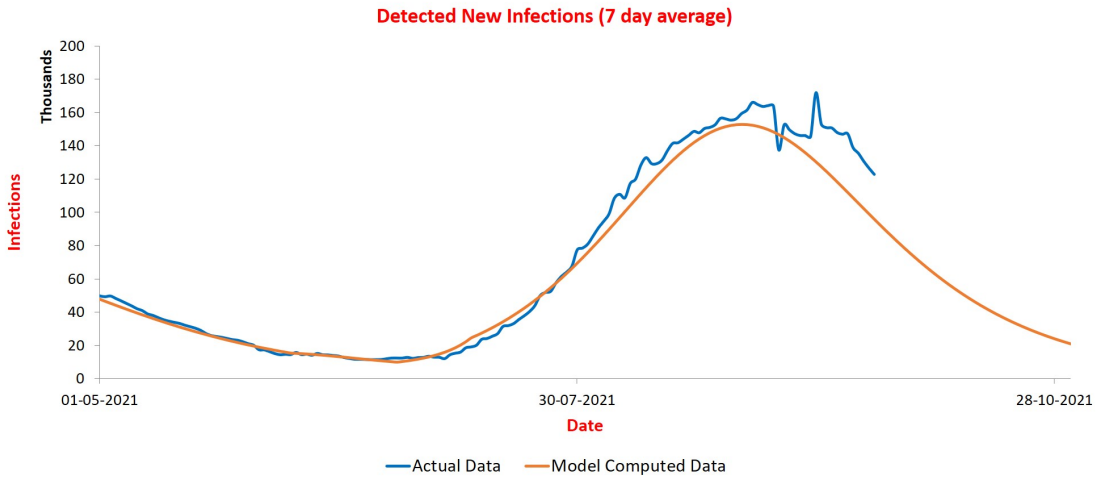


Figure 2: Predicted US Trajectory on 25th July 2021 versus actual

And finally, parameter estimation allows us to compute trajectories of the pandemic for detected infections as well as total infections. We also show that there is a *unique canonical trajectory* for total infections corresponding to a trajectory for detected infections given a set of initial conditions.

## 2 Literature Review

There is a vast literature on the modelling of epidemics. A comprehensive review [15] published in the year 2000 already had 200+ references. Book length treatments are available in [1, 9, 18, 3, 25]. Historically the first epidemiological model is the SIR model introduced in [19], given by

$$\dot{S} = -\beta IS, \dot{I} = \beta IS - \gamma I, \dot{R} = \gamma I, \quad (1)$$

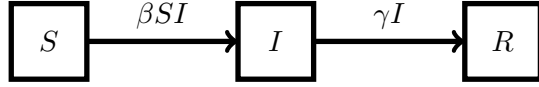


Figure 3: Flowchart of the SIR model

where  $S, I, R$  denote respectively the fraction of the population that is Susceptible, Infected, and Removed.<sup>1</sup> Note that  $S + I + R = 1$ . Consequently  $S(t) + I(t) = R(t) = 1$  for all  $t$ . Therefore we can ignore any one of the three equations and focus only on the other two. Most authors ignore  $R$  and study

$$\dot{S} = -\beta IS, \dot{I} = \beta IS - \gamma I, \quad (2)$$

where  $\beta, \gamma > 0$  are parameters of the disease under study. Specifically,  $\beta$  is called the “contact rate parameter” and represents the likelihood that contact between a susceptible individual and an infected individual leads to a fresh infection, while  $\gamma$  denotes the rate at which infected persons get removed. In principle, there should be a time delay in the above equations (2), in the form

$$\dot{S}(t) = -\beta I(t - \Delta)S(t - \Delta), \dot{I}(t) = \beta I(t - \Delta)S(t - \Delta) - \gamma I(t),$$

where  $\Delta$  denotes the incubation period of the virus in an infected person. However, it is shown in [1, 18] that, other than complicating the solution of the equations, the time delay does not change the *qualitative* behavior of the solutions. Therefore practically all researchers do not introduce such a delay, and neither do we. A compartmental diagram depicting the above flow is given in Figure 3.

The ratio  $R_0 := \beta/\gamma$  is called the **basic reproduction ratio**. Its significance lies in the fact that if  $R_0 S(0) < 1$ , then  $\dot{I} < 0$  for all times, and the pandemic does not grow. If  $R_0 S(0) > 1$ , then  $I(t)$  increases initially and reaches its maximum value when  $\dot{I} = 0$ , or  $S = \gamma/\beta = 1/R_0$ . Since  $S + I + R = 1$  at all times, it follows that when  $I$  reaches its maximum, the value of  $I + R$  equals  $1 - 1/R_0 = (R_0 - 1)/R_0$ , a number often referred to as the **herd immunity level**. The introduction of the phrase “herd immunity” predates the first SIR model and is found in [33]. However, it took several decades for a precise mathematical formulation of this concept, and the discovery of the formula  $(R_0 - 1)/R_0$ . This formula is derived in [31, 10]. The reader is directed to and to [11] for a historical overview of how this concept has developed over time.

While the above SIR model is a good starting point, a more realistic model consists of an intermediate group called  $E$  (for Exposed) in-between  $S$  and  $I$ . The equations for the SEIR model, which are studied in [21, 20] are as follows:

$$\dot{S} = -\beta IS, \dot{E} = \beta IS - \gamma E, \dot{I} = \gamma E - \delta I, \dot{R} = \delta I. \quad (3)$$

The above equations mean that when a person from group  $S$  comes into contact with a person from group  $I$ , then the former becomes “exposed” at a rate of  $\beta$ . Note that the transition is out of group  $S$  but to group  $E$ , and not to group  $I$ . The persons in group  $E$  become infected at a rate  $\gamma$ , and move to group  $I$ . Finally, people in group  $I$  move to group  $R$  at a rate of  $\delta$ . Note that the transition of people is strictly sequential in the order  $S \rightarrow E \rightarrow I \rightarrow R$ . Also that there is no term of the form  $ES$  in the above equations. Therefore, contact between a susceptible person and an exposed person does not have any consequences. This is *precisely* the difference between previous

<sup>1</sup>Some authors use the letter  $R$  to denote “Recovered,” which presupposes that no one dies. It is more realistic to use the phrase “Removed” that includes both those who recover and those who die.

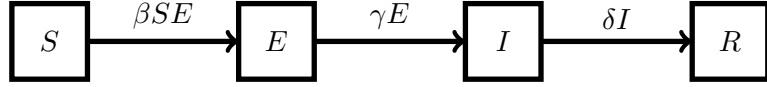


Figure 4: Flowchart of the SEIR model

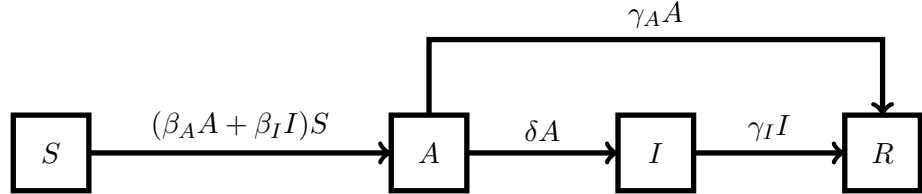


Figure 5: Flowchart of the SAIR model

diseases to which the SEIR model has been applied, and COVID-19. A compartmental diagram of the SEIR model is given in Figure 4.

Apparently the first paper to identify asymptomatic patients as a separate category is [30]. The model proposed there, which might be called the SAIR model, is as follows: The population is divided into four groups, denoted as Susceptible ( $S$ ), Asymptomatic ( $A$ ), Infected ( $I$ ), and Removed ( $R$ ).

$$\begin{aligned}
 \dot{S} &= -\beta_A AS - \beta_I IS, \\
 \dot{A} &= \beta_A AS + \beta_I IS - \gamma_A A - \delta A, \\
 \dot{I} &= \delta A - \gamma_I I, \\
 \dot{R} &= \gamma_A A + \gamma_I I.
 \end{aligned} \tag{4}$$

In contrast with the SEIR model of (3), in the SAIR model, interactions between susceptible persons ( $S$ ) on one side, and *either asymptomatic ( $A$ ) or infected ( $I$ ) persons* on the other side, can lead to fresh infections, at rates of  $\beta_A$  and  $\beta_I$  respectively. The newly infected persons initially enter the asymptomatic group  $A$ . The asymptomatic persons in the  $A$  group move to the  $I$  group and become symptomatic at a rate of  $\delta$ , while others recover by moving to the group  $R$  at a rate of  $\gamma_A$ . directly to the  $R$  group rate at another rate. Finally, symptomatic persons in the  $I$  group get removed at a rate of  $\gamma_I$ . A compartmental diagram depicting the SAIR model is given in Figure 5.

Several refinements of these basic models above have been studied in the literature. These can be grouped into two broad categories. First, one can introduce births and deaths, often referred to as “vital dynamics.” Second, one can introduce a feature whereby people who enter the  $R$  group return to the susceptible group  $S$  at some predetermined rate. This leads to models known as SIRS, SEIRS, and SAIRS (though the last one does not appear to have been studied. In each case, the disease remains *endemic* in the sense that  $I(t)$  does not converge to zero, but a positive value. The interested reader is referred to the survey paper [15] or [2] for further details.

None of the existing models have been able to capture the trajectory of COVID-19 pandemic well. This has been due to the complex nature of the pandemic and frequent interventions made to control it. It has led to creating of several new models with additional groups and parameters [13, 12].

### 3 The SUTRA Model

While the SAIR model formulated in [30] is the first one to make a clear distinction between asymptomatic and symptomatic patients, it does make one unrealistic assumption, namely: that *all* symptomatic persons get detected. The logic in [30] is that persons with symptoms would present themselves to the health authorities, while asymptomatic persons would not. Over time, some asymptomatic patients would develop symptoms, at which time they too would present themselves to the health authorities. However, this is not how matters have evolved during the COVID-19 pandemic. Instead of the  $A$  and  $I$  groups, it is more realistic to have groups  $U$  for Undetected but infected, and  $T$  for Tested Positive. One would expect both the groups to consist of a mix of symptomatic and asymptomatic cases, since many asymptomatic cases get detected due to contact tracing and many symptomatic cases do not get tested. We adopt this approach (similar approach is used in some recent papers too, e.g. [13]).

Let us now construct a model for the evolution of the pandemic. It is a *mean-field* model, that ignores heterogeneity in the population and works with average values of all parameters.

As is the convention, we use letters  $S$ ,  $U$ ,  $T$ ,  $R_U$ , and  $R_T$  to denote the fraction of population in the five groups of same name respectively. Here  $R_U$  and  $R_T$  denote the group of removed cases from  $U$  and  $T$  respectively.

At present, in most countries, persons in the group  $T$  (whether symptomatic or not) are quarantined, and it can be assumed that they do not come into contact with the susceptible population  $S$ . Therefore persons in group  $S$  get infected only through contact with group  $U$  of undetected infected patients, with a likelihood of  $\beta$ . Finally, it is obvious that all infected persons are initially undetected, and thus enter group  $U$ . In turn some part of  $U$ , call it  $N_T$ , gets tested positive and moves to  $T$ , while another part moves towards recovery. This leads to

$$\begin{aligned}\dot{S} &= -\beta SU, \dot{U} = \beta SU - N_T - \gamma_U U \\ \dot{T} &= N_T - \gamma_T T, \dot{R}_U = \gamma_U U, \dot{R}_T = \gamma_T T.\end{aligned}$$

where  $\gamma_U$  is the rate of removal from  $U$ , and  $\gamma_T$  is the rate of removal from  $T$ .

Although removal rates for symptomatic ( $= \gamma_I$ ) and asymptomatic ( $= \gamma_A$ ) groups are reported to differ by a few days [4], removal rates for  $U$  ( $= \gamma_U$ ) and  $T$  ( $= \gamma_T$ ) groups are much closer:

**Lemma 1.** *Let  $f$  be the fraction of symptomatic cases in  $T$  and  $g$  be the fraction of symptomatic cases in  $U$ . Then,*

$$\gamma_T - \gamma_U = (f - g) \cdot (\gamma_I - \gamma_A).$$

*Proof.* We have  $\gamma_T = f\gamma_I + (1 - f)\gamma_A$  and  $\gamma_U = g\gamma_I + (1 - g)\gamma_A$ . Therefore,  $\gamma_T - \gamma_U = (f - g) \cdot (\gamma_I - \gamma_A)$ .  $\square$

We can assume that  $f > g$  since symptomatic patients are more likely to get tested. In case  $f$  and  $g$  do not differ by much (in US [5],  $f - g < 1/8$ ) or  $f$  is significantly smaller than 1 (in India [28],  $f < 1/10$ ),  $\gamma_T \approx \gamma_U$  since  $\gamma_I - \gamma_A$  is not more than five days [4, 8].

Above justifies the following simplification:

$$\gamma_U = \gamma_T = \gamma.$$

The equations then simplify to:

$$\begin{aligned}\dot{S} &= -\beta SU, \dot{U} = \beta SU - N_T - \gamma U \\ \dot{T} &= N_T - \gamma T, \dot{R}_U = \gamma U, \dot{R}_T = \gamma T.\end{aligned}$$

Thus the model formulation is complete once we specify  $N_T$ , the fraction tested positive at time  $t$ . One possibility is to assume that everyone in  $U$  is equally likely to get detected, so that  $N_T = \delta U$ , for some  $\delta > 0$ . This would lead to

$$\dot{U} = \beta SU - \delta U - \gamma U, \dot{T} = \delta U - \gamma T.$$

This is the same as the SAIR model in Equation (4) with  $\beta_A = \beta_I$  and  $\gamma_A = \gamma_I$ , and  $A$  and  $I$  replaced by  $U$  and  $T$  respectively. However, detection of COVID-19 cases is biased towards more recently infected due to contact tracing. Divide  $T$  into two subgroups:  $T_C$  containing those that are detected through contact tracing and  $T_{NC}$  are the rest.

**Lemma 2.** *Suppose an infected person infects  $R_0$  other persons. Further, suppose that upon detection of a positive case, all who came in contact with the infected person are also tested. Then, the expected number of days a person in  $T$  stays in  $U$  is  $\frac{R_0+2}{2(R_0+1)}k$ , where  $k$  is the average number of days a person in  $T_{NC}$  stays in  $U$ .*

*Proof.* Observe that  $|T_C| = \frac{1}{R_0+1}|T|$  since for every initiating case, contact tracing will find  $R_0$  additional cases on average. The cases detected via contact tracing would be infected after the initiating case, and therefore, between 1 and  $k-1$  days ago. These are expected to be uniformly distributed in the range  $[1, k-1]$  and therefore, the expected number of days a person in  $T$  stays in  $U$  equals:

$$\begin{aligned} pk + \sum_{i=1}^{k-1} \frac{1-p}{k-1} i &= pk + \frac{1-p}{2} k \\ &= \frac{1+p}{2} k \\ &= \frac{R_0+2}{2(R_0+1)} k \end{aligned}$$

□

The mean duration for which a symptomatic case remained infected was estimated to be around 13.4 in [4]. However, the movement from  $T$  to  $R_T$  is likely to happen earlier since a person may stop infecting others while still being RTPCR positive (this number is estimated to be less than 10 days for symptomatic cases in [8]). Average duration of stay in  $U$  for a person in  $T_C$  is likely to be less than half of above duration, so  $k$  is less than 5. For Covid-19, the values of  $R_0$  has been estimated to be in the range [3, 6] depending on the mutant. Therefore, the expected number of days a person in  $T$  stays in  $U$  is less than 4.

Above analysis shows that the cases that move from  $U$  to  $T$  are significantly biased towards recently infected ones, and therefore, it is better to set  $N_T$  to be proportional to a fraction of recently infected cases. This number can be taken to be proportional to  $\beta SU$ , the fraction of persons who got infected *most recently*, as the number of cases do not change significantly over a window of few days. Therefore we choose  $N_T = \epsilon \beta SU$ , with  $\epsilon$  being another parameter of the model. With this assumption, the full SUTRA model becomes

$$\dot{S} = -\beta SU, \tag{5}$$

$$\dot{U} = \beta SU - \epsilon \beta SU - \gamma U, \dot{T} = \epsilon \beta SU - \gamma T, \tag{6}$$

$$\dot{R}_U = \gamma U, \dot{R}_T = \gamma T. \tag{7}$$

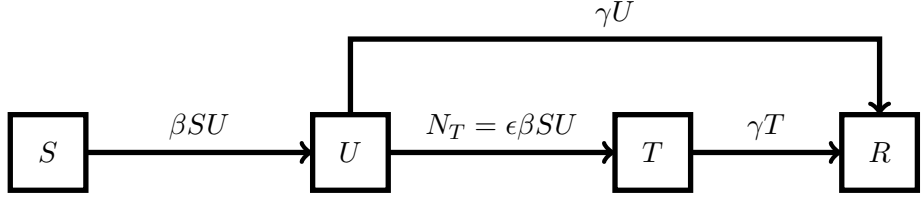


Figure 6: Flowchart of the SUTRA model

A compartmental diagram depicting the SUTRA model is given in Figure 6.

The acronym SUTRA stands for Susceptible, Undetected, Tested (positive), and Removed (recovered or dead) Approach. Susceptible, The word Sutra also means an aphorism. Sutras are a genre of ancient and medieval Hindu texts, and depict a code strung together by a genre.

It is possible to introduce another parameter  $D$  denoting deaths, and write it as  $\dot{D} = \eta T$ . However, it is quite easy to estimate  $\eta$  as the ratio between the incremental death totals and the increase in cumulative positive test cases. Hence that relationship is not shown as a part of the SUTRA model.

## 4 Analyzing Model Equations

Defining  $M = U + T$ ,  $R = R_U + R_T$ , we get from equations (6) and (7) that

$$\dot{M} + \dot{R} = \beta SU = \frac{1}{\epsilon}(\dot{T} + \dot{R}_T), \quad (8)$$

resulting in

$$M + R = \frac{1}{\epsilon}(T + R_T) + c \quad (9)$$

for an appropriate constant of integration  $c$ . Adding equations (6) gives

$$\dot{M} = \beta SU - \gamma M = \frac{1}{\epsilon}(\dot{T} + \gamma T) - \gamma M,$$

or

$$\frac{d(Me^{\gamma t})}{dt} = \frac{1}{\epsilon} \frac{d(Te^{\gamma t})}{dt}, \quad (10)$$

resulting in

$$M = \frac{1}{\epsilon}T + de^{-\gamma t} \quad (11)$$

for some constant  $d$ . Since  $e^{-\gamma t}$  is a decaying exponential, it follows that, except for an initial transient period, the relationship  $M = \frac{1}{\epsilon}T$  holds. This in turn implies that  $U = M - T = \frac{1-\epsilon}{\epsilon}T$ . How long is the transient period? Observe that the constant  $d$  equals  $M(0) - \frac{1}{\epsilon}T(0)$  which is close to zero since fraction of infected cases at the start of pandemic is very small. Therefore the transient period will not last more than a few days. As we will see later, such transient periods will recur at various stages of pandemic and all of them remain small.

These simplifications allow us to rewrite equation (8) as:

$$\begin{aligned}
N_T &= \epsilon\beta SU = \beta(1 - \epsilon)ST \\
&= \beta(1 - \epsilon)(1 - (M + R))T \\
&= \beta(1 - \epsilon)\left(1 - \frac{1}{\epsilon}(T + R_T) - c\right)T \\
&= \beta(1 - \epsilon)(1 - c)T - \frac{\beta(1 - \epsilon)}{\epsilon}(T + R_T)T
\end{aligned} \tag{12}$$

Rearrange (12) as

$$T = \frac{1}{\tilde{\beta}}N_T + \frac{1}{\epsilon(1 - c)}(T + R_T)T, \tag{13}$$

where

$$\tilde{\beta} = \beta(1 - \epsilon)(1 - c).$$

## 5 Discretization of the Model Relationships

The progression of a pandemic is typically reported via two daily statistics: The number of people who test positive, and the number of people who are removed (including both recoveries and deaths). The second statistics has a problem though: there is no agreement on when to classify an infected person as removed. Some do it when RTPCR test is negative, some do it when symptoms are gone for a certain period, and some others do it after a fixed period of time. For the purpose of modeling, this classification needs to be done at the time when an infected person is no longer capable of infecting others. This is hard to decide, and so is almost never done. Further, some countries do not report second statistics at all (UK for example). In such a situation, we do not rely on reported data, and instead compute  $R_T$  by fixing  $\gamma$  to an appropriate value as discussed in section on parameter estimation.

Let  $\mathcal{T}(t)$  denote the number of detected cases who are capable of infecting others on day  $t$ ,  $\mathcal{R}_T(t)$  denote the number of detected cases that are removed on or before day  $t$ , and  $\mathcal{N}_T(t)$  denote the number of cases detected on day  $t$ . Note that, in this notation, all three are integers, and  $t$  is also a discrete counter. In contrast, in the SUTRA model,  $T$ ,  $R_T$  and  $N_T$  are *fractions* in  $[0, 1]$ , while  $t$  is a continuum. In order to infer these *fractions* from the *case numbers*, we observe that

$$T = \frac{\mathcal{T}}{P}, R_T = \frac{\mathcal{R}_T}{P}, N_T = \frac{\mathcal{N}_T}{P}$$

where  $P$  is the *effective population* that is potentially affected by the pandemic. Now we introduce the parameter measuring the spread of the pandemic. We define a number  $\rho$ , called the “reach,” which equals  $P/P_0$ , where  $P$  is the effective population and  $P_0$  is the *total population* of the group under study, e.g., the entire country, or an individual state, or a district (this parameter is also introduced and studied in [12]). The reach parameter  $\rho$  is usually nondecreasing, starts at 0, and increases towards 1 over time (situations where it decreases are discussed later). While the underlying population  $P_0$  is known, the reach  $\rho$  is not known and must be inferred from the data.

Substituting  $P = \rho P_0$ ,

$$\mathcal{T} = PT = \rho P_0 T, \mathcal{R}_T = PR_T = \rho P_0 R_T, \mathcal{N}_T = PN_T = \rho P_0 N_T$$

into (13) gives a relationship that involves *only measurable and computable quantities*  $\mathcal{T}$ ,  $\mathcal{R}_T$  and  $\mathcal{N}_T$ , and the parameters of the model, namely

$$\mathcal{T} = \frac{1}{\tilde{\beta}} \mathcal{N}_T + \frac{1}{\tilde{\rho} P_0} (\mathcal{T} + \mathcal{R}_T) \mathcal{T}, \quad (14)$$

where

$$\tilde{\rho} = \epsilon \rho (1 - c).$$

Eq. (14) is the *fundamental equation* governing the pandemic. It establishes a relationship between  $\mathcal{N}_T$ ,  $\mathcal{T}$ , and  $(\mathcal{T} + \mathcal{R}_T) \mathcal{T}$ , first of which is directly measurable and the remaining two are computable once  $\gamma$  is fixed.

Finally, since  $\mathcal{T}$ ,  $\mathcal{R}_T$  and  $\mathcal{N}_T$  are available at only discrete time instants, we first turn (14) into an integral relationship by integrating both sides over an interval  $[t - \Delta, t]$ , where we take  $\Delta$  to equal seven days. This is because reported daily case numbers usually have a weekly periodicity to them. This gives

$$\begin{aligned} \int_{t-\Delta}^t \mathcal{T}(s) ds &= \frac{1}{\tilde{\beta}} \int_{t-\Delta+1}^{t+1} \mathcal{N}_T(s) ds \\ &+ \frac{1}{\tilde{\rho} P_0} \int_{t-\Delta}^t [\mathcal{T}(s) + \mathcal{R}_T(s)] \mathcal{T}(s) ds. \end{aligned} \quad (15)$$

Note that integration for  $\mathcal{N}_T$  is shifted forward by one day since new infections reported on day  $t + 1$  are determined by active infections and susceptible population on day  $t$ .

## 6 Phase Changes

The parameters  $\rho$ ,  $\beta$  and  $\epsilon$  are not constant, and vary over time. In the case of the reach parameter  $\rho$ , it increases in spurts, for example when the pandemic hits a new region.

In the case of the contact rate  $\beta$ , it changes for following reasons:

- Emergence of new and more infectious variants of the virus, which would spread faster than its predecessor. It takes time for the new variant to overtake whatever existed previously, which is why this factor would cause  $\beta$  to increase over a period.
- Non-compliance with COVID guidelines. The  $\beta$  parameter measures the likelihood of infection when an infected person (from either  $U$  or  $T$ ) meets a susceptible person from  $S$ . Thus  $\beta$  increases if people do not wear masks, or fail to maintain social distancing, and the like.
- The parameter can also *decrease* suddenly, with almost a step change, due to non-pharmaceutical interventions such as lockdowns.

Finally, the  $\epsilon$  parameter, which equals the ratio  $T/(U + T)$ , can increase due to more comprehensive testing. The presumption is that more testing will increase  $T$  without increasing the total pool  $U + T$ .

The changes in parameter values occur either as a slow drift over extended period of time, or as sudden rise and fall. We divide the entire timeline of the pandemic into *phases*, such that within each phase, the parameters are (nearly) constant. A *phase change* occurs when one of the parameter values changes significantly. It could be due to a quick change for reasons listed above, or accumulated slow change over an extended period. By convention, we include the duration of

change in a parameter as part of new phase and call it *drift period* of the phase. The remaining duration of a phase is called *stable period* of the phase.

When the value of  $\epsilon$  changes, then the relationship  $T = \epsilon M$  breaks down for certain period. When  $\epsilon$  stabilizes to its new value,  $T$  converges to  $\epsilon M$  after some time. How long will this duration be? Following lemma helps us estimate it.

**Lemma 3.** *Suppose a new phase begins at time  $t_0$  with a drift period of  $t_1 - t_0$ . Then,*

$$|\mathcal{M}(t_1) - \frac{1}{\epsilon(t_1)}\mathcal{T}(t_1)| \lesssim \frac{|\epsilon(t_1) - \epsilon(t_0)|}{\epsilon(t_0)} \frac{1}{\epsilon(t_1)} \mathcal{T}(t_1)$$

provided  $\mathcal{T}(t) \geq \frac{1}{e^\gamma} \mathcal{T}(t-1)$  for the duration.

*Proof.* Integrating equation (8) over the drift period, we get:

$$\begin{aligned} \mathcal{M}(t_1)e^{\gamma(t_1-t_0)} &= \mathcal{M}(t_0) + e^{-\gamma t_0} \int_{t_0}^{t_1} \frac{1}{\epsilon(t)} d(\mathcal{T}(t)e^{\gamma t}) \\ &\approx \mathcal{M}(t_0) + e^{-\gamma t_0} \sum_{t=t_0+1}^{t_1} \frac{1}{\epsilon(t)} (\mathcal{T}(t)e^{\gamma t} - \mathcal{T}(t-1)e^{\gamma(t-1)}) \\ &= \frac{1}{\epsilon(t_1)} \mathcal{T}(t_1)e^{\gamma(t_1-t_0)} + \sum_{t=t_0+1}^{t_1} \left( \frac{1}{\epsilon(t-1)} - \frac{1}{\epsilon(t)} \right) \mathcal{T}(t-1)e^{\gamma(t-1-t_0)}. \end{aligned}$$

Therefore,

$$\begin{aligned} |\mathcal{M}(t_1) - \frac{1}{\epsilon(t_1)}\mathcal{T}(t_1)| &\lesssim \sum_{t=t_0+1}^{t_1} \left| \frac{1}{\epsilon(t-1)} - \frac{1}{\epsilon(t)} \right| \mathcal{T}(t-1)e^{-\gamma(t_1+1-t)} \\ &\leq \left| \frac{1}{\epsilon(t_1)} - \frac{1}{\epsilon(t_0)} \right| \mathcal{T}(t_1) \\ &= \frac{|\epsilon(t_1) - \epsilon(t_0)|}{\epsilon(t_0)} \frac{1}{\epsilon(t_1)} \mathcal{T}(t_1) \end{aligned}$$

where the second inequality uses the assumption that  $\mathcal{T}(t-1)e^{-\gamma} \leq \mathcal{T}(t)$ . □

It has been observed that the value of  $\epsilon$  does not change significantly from one phase to next (due to testing strategy not changing in a major way over a short period), and active cases almost never decline by more than 10% in one day, and so  $\mathcal{T}(t) \geq \mathcal{T}(t-1)/1.1 > \mathcal{T}(t-1)e^{-\gamma}$ . Therefore,  $|\epsilon(t_1) - \epsilon(t_0)|/\epsilon(t_0)$  will be significantly smaller than one, which implies that  $\mathcal{M} \approx \frac{1}{\epsilon} \mathcal{T}$  already by the end of drift period.

## 7 Detected Trajectory of Pandemic

Daily values of  $\mathcal{N}_T$  over a given time period define *detected trajectory*. Following algorithm computes parameter values for different phases given  $\mathcal{N}_T$  over a time period.

```

Input:  $\mathcal{N}_T(t)$ , for  $1 \leq t \leq t_e$ ,  $\mathcal{T}(0)$ ,  $\mathcal{R}_T(0)$ ,  $P_0$ , and  $t_p$ 
/*  $t_e$  : last date for which data is available
 *  $P_0$  : population,  $t_p$  : last date for simulation
 */

1. Fix  $\gamma = 0.1$ ;
2. Set  $t = 1$ ;
3. while  $t < t_e$  do the following:
   (a) Find drift and stable periods of the phase starting at day  $t$ ;
   (b) Compute values  $\tilde{\beta}$  and  $\tilde{\rho}$  for the phase;
   (c) Increase  $t$  to day after the end of the phase;
4. Compute and output the detected trajectory of the pandemic until  $t_p$ ;

```

In the following subsections we provide details of the algorithm along with necessary justifications.

## 7.1 Fixing $\gamma$

As discussed in the previous section, reported removal data does not provide a good estimate for  $\gamma$ . In [4], median duration of infection for asymptomatic cases was estimated in the range [6.5, 9.5] and mean duration for symptomatic cases in the range [10.9, 15.8] days with a caveat that the duration reduces when children are included. In [8], infection duration for symptomatic cases is observed to be less than 10 days. Since our groups  $U$  and  $T$  consist of a mix of asymptomatic and symptomatic cases, and it is likely that an infected person stops infecting others before becoming RTPCR negative, we take the mean duration of infection for both groups to be 10 days. This implies  $\gamma = 0.1$ .

All our simulations are done using the above value of  $\gamma$  and show a good fit with the actual trajectories.

## 7.2 Finding a Phase and Estimating Its Parameter Values

We use equation (15) for computing the duration of current phase, its drift period, and associated parameter values  $\tilde{\beta}$  and  $\tilde{\epsilon}$ .

Consider first  $m$  days from the starting day of the current phase. From the input data  $\mathcal{N}_T$  and using the value  $\gamma = 0.1$ , we can compute  $\mathcal{T}$  and  $\mathcal{R}_T$  values for the period. Represent values of  $\int_{t-\Delta}^t \mathcal{T}(s)ds$ ,  $\int_{t-\Delta+1}^{t+1} \mathcal{N}_T(s)ds$ , and  $\int_{t-\Delta}^t (\mathcal{T}(s) + \mathcal{R}_T(s))\mathcal{T}(s)ds$  ( $\Delta = 7$ ) for this period by  $m$ -dimensional vectors  $\mathbf{u}$ ,  $\mathbf{v}$ , and  $\mathbf{w}$  respectively. Equation (15) can be rewritten for the period as:

$$\mathbf{u} = \frac{1}{\tilde{\beta}} \mathbf{v} + \frac{1}{\tilde{\rho} P_0} \mathbf{w}.$$

The values of  $\tilde{\beta}$  and  $\tilde{\rho}$  can be estimated using standard linear regression. If  $R^2$ -value of the estimate is not very high, it indicates that either a phase change has occurred within  $m$  days or drift period of the current phase is bigger than  $m$ . In either case,  $m$  needs to be changed. Repeat this until a high  $R^2$ -value ( $\geq 0.98$ ) is obtained. This gives a good estimate of parameter values of the phase.

The phase may extend beyond  $m$  days though; so to detect phase boundary, we increase  $m$  until  $R^2$ -value of the fit reduces. This algorithm is captured below.

```

Input:  $\mathcal{N}_T(t)$ , for  $t_0 \leq t \leq t_e$ ,  $\mathcal{T}(0)$ ,  $\mathcal{R}_T(0)$ ,  $P_0$ 
/*  $t_0$ : starting date of the phase
 *  $t_e$ : last date for which data is available,  $P_0$ : population
 */

1. Set  $R^2 = 0.0$ ;  $m = 10$ ;
2. while  $R^2 < 0.98$  do the following:
   (a) Compute vectors  $\mathbf{u}$ ,  $\mathbf{v}$  and  $\mathbf{w}$  from data  $\mathcal{N}_T(t_0)$ , ...,  $\mathcal{N}_T(t_0 + m)$ ;
   (b) Use linear regression to compute  $\tilde{\beta}$  and  $\tilde{\rho}$ , and its  $R^2$ -value;
   (c) If  $R^2 < 0.98$ , set  $m = m + 1$ ;
   (d) If  $t_0 + m > t_e$ , exit with error;
3. Increase  $m$  and repeat until  $R^2$ -value becomes  $< 0.98$  or  $t_0 + m = t_e$ ;

```

### 7.2.1 Linear Regression

The standard way is to find values for  $\tilde{\beta}$  and  $\tilde{\epsilon}$  that maximize the  $R^2$ -value given by

$$R^2 = 1 - \frac{|\mathbf{u} - \frac{1}{\tilde{\beta}}\mathbf{v} - \frac{1}{\tilde{\epsilon}}\mathbf{w}|^2}{|\mathbf{u}|^2},$$

where  $|\cdot|$  denotes the Euclidean norm of a vector.

When there are relatively few data points in a phase (which happens when the duration of the phase is short), or the data has significant errors, standard linear regression method fails to work at times (estimated parameter value becomes negative). In such situations we use a different method for estimation that is more tolerant to errors as described below.

Let

$$R_\beta^2 = 1 - \frac{|\mathbf{u} - \frac{1}{\tilde{\beta}}\mathbf{v} - \frac{1}{\tilde{\epsilon}}\mathbf{w}|^2}{|\mathbf{u} - \frac{1}{\tilde{\epsilon}}\mathbf{w}|^2}$$

$$R_\epsilon^2 = 1 - \frac{|\mathbf{u} - \frac{1}{\tilde{\beta}}\mathbf{v} - \frac{1}{\tilde{\epsilon}}\mathbf{w}|^2}{|\mathbf{u} - \frac{1}{\tilde{\beta}}\mathbf{v}|^2}$$

Find values of  $\tilde{\beta} > 0$  and  $\tilde{\epsilon} > 0$  that maximize the product  $R^2 = R_\beta^2 \cdot R_\epsilon^2$ . This choice ensures that both  $\tilde{\beta}$  and  $\tilde{\epsilon}$  play almost equally significant roles in minimizing the error. Further, the desired maximum of  $R_\beta^2 R_\epsilon^2$  is guaranteed to exist:

**Lemma 4.** *When  $\mathbf{u}$  is independent of  $\mathbf{v}$  as well as  $\mathbf{w}$ , there is a maxima of  $R^2$  with  $R_\beta^2, R_\epsilon^2, \tilde{\beta}, \tilde{\rho} > 0$ .*

*Proof.* Let  $x = \frac{1}{\tilde{\beta}}$  and  $y = \frac{1}{\tilde{\rho}}$ . Then we have:

$$R^2 = \frac{xy(2\mathbf{v}^T \mathbf{u} - y\mathbf{v}^T \mathbf{w} - x\mathbf{v}^T \mathbf{v})(2\mathbf{w}^T \mathbf{u} - x\mathbf{w}^T \mathbf{v} - y\mathbf{w}^T \mathbf{w})}{|\mathbf{u} - y\mathbf{w}|^2 |\mathbf{u} - x\mathbf{v}|^2} \quad (16)$$

with  $R_\beta^2 > 0$  iff  $2\mathbf{w}^T \mathbf{u} - x\mathbf{w}^T \mathbf{v} - y\mathbf{w}^T \mathbf{w} > 0$  and  $R_\epsilon^2 > 0$  iff  $2\mathbf{v}^T \mathbf{u} - y\mathbf{v}^T \mathbf{w} - x\mathbf{v}^T \mathbf{v} > 0$ .

The denominator of equation (16) is always positive since  $\mathbf{u}$  is independent of  $\mathbf{v}$  as well as  $\mathbf{w}$ . The numerator is a product of four linear terms in the unknowns  $x$  and  $y$ . Therefore the value of  $R^2$  is positive inside the polygon defined by:

$$\begin{aligned} x &\geq 0 \\ y &\geq 0 \\ 2\mathbf{v}^T \mathbf{u} - y\mathbf{v}^T \mathbf{w} - x\mathbf{v}^T \mathbf{v} &\geq 0 \\ 2\mathbf{w}^T \mathbf{u} - x\mathbf{w}^T \mathbf{v} - y\mathbf{w}^T \mathbf{w} &\geq 0 \end{aligned}$$

and is zero on the boundaries. This guarantees that there exists at least one maxima inside the polygon.  $\square$

The only situation when the above method will not yield the desired maxima of  $R^2$  is when  $\mathbf{u}$  is dependent on either  $\mathbf{v}$  or  $\mathbf{w}$ . Former implies that  $\mathcal{T}$  is proportional to  $\mathcal{N}_T$  for  $m$  days, or equivalently,  $S$  does not change over the period. This implies  $\mathcal{N} = 0 = \mathcal{N}_T = \mathcal{T}$  for the period. Similarly, latter implies that  $\mathcal{T}$  is proportional to  $(\mathcal{T} + \mathcal{R}_T)\mathcal{T}$  for  $m$  days, or equivalently,  $\mathcal{T} + \mathcal{R}_T$  does not change over the period. This also implies that  $\mathcal{N}_T = 0 = \mathcal{N}$ . Either case occurs when the pandemic has effectively ended and there are no new cases for an extended period.

### 7.2.2 Error Estimates for Parameters

The uncertainty in the parameter estimation is computed using the standard mean-square error formula for linear regression. We use it to compute 95% confidence interval ranges for  $\tilde{\beta}$  and  $\tilde{\rho}$  values.

### 7.2.3 Identifying Drift Period and Fine-tuning Phase Boundaries

While the algorithm above detects phase boundaries reasonably well, it can be improved with manual intervention. Such intervention is also required to identify drift period of the phase since a point could also appear in drift period due to error in data. In this subsection, we show how to do this through a few examples for India.

To visualize how well is equation (15) satisfied, we plot points

$$\mathcal{P}(t) = \left( \int_{t-7}^t \mathcal{T}(s)ds - \frac{1}{\tilde{\beta}} \int_{t-7}^t \mathcal{N}_T(s)ds, \frac{1}{P_0} \int_{t-7}^t (\mathcal{T}(s) + \mathcal{R}_T(s))\mathcal{T}(s)ds \right) \quad (17)$$

for  $t_0 \leq t < t_0 + m$  for estimated value of  $\tilde{\beta}$ . It is straightforward to see that (15) holds if and only if above points lie on a straight line passing through the origin with a slope of  $\frac{1}{\tilde{\beta}}$ .

Let us start with points  $\mathcal{P}(t)$  for  $t$  between March 23 to May 23, 2020. This was the beginning of the pandemic in India. The plot in Figure 7 shows these points with regression provided values of  $\tilde{\beta} \approx 0.19$ ,  $\frac{1}{\tilde{\rho}} \approx 4469.7$ , and  $R^2 \approx 0.96$ . It is clear that the points in the beginning lie on a very different line than last twenty odd ones, indicating a phase change in April-end. Indeed, the simulation (Figure 8) is way off the actual trajectory.

Removing points after April 30 gives values  $\tilde{\beta} \approx 0.27$ ,  $\frac{1}{\tilde{\rho}} \approx 23870.9$ , and  $R^2 \approx 0.98$ . Now the fit is much better, but points show a slow drift (Figure 9). The simulation has improved significantly, but is still not fitting well due to the drift (Figure 10).

Removing ten more points reduces the drift (Figure 11), with  $\tilde{\beta} \approx 0.29$ ,  $\frac{1}{\tilde{\rho}} \approx 54245.9$ , and  $R^2 \approx 0.99$ . The simulation shows an excellent fit (Figure 12).

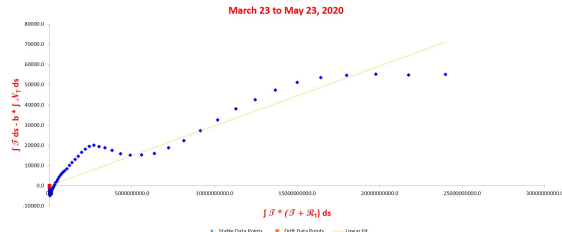


Figure 7: India Phase Plot

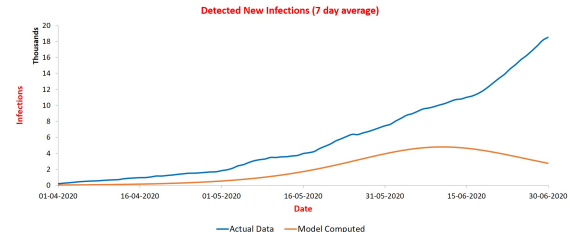


Figure 8: India Trajectory



Figure 9: India Phase Plot

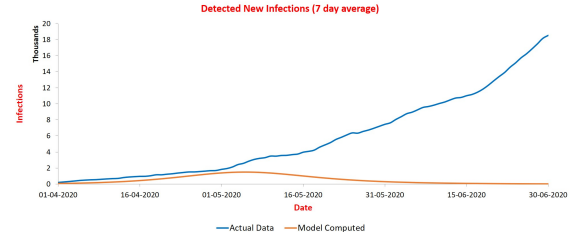


Figure 10: India Trajectory

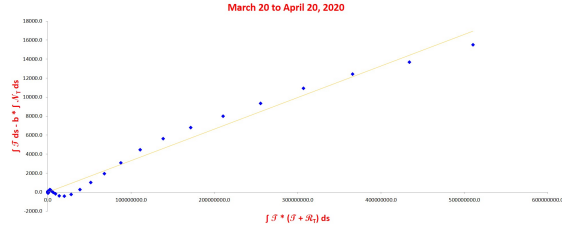


Figure 11: India Phase Plot

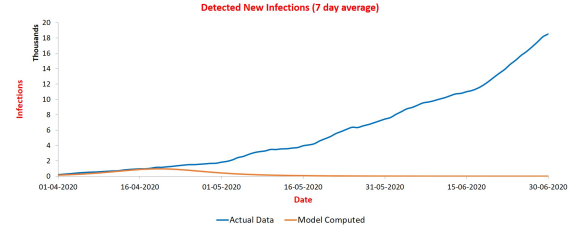


Figure 12: India Trajectory

We start a new phase from April 21st and plot points up to June 30th. Again, last ten points show a clear deviation from the trajectory of previous points in Figure 13 ( $\tilde{\beta} \approx 0.16$ ,  $\frac{1}{\tilde{\rho}} \approx 785.3$ ,  $R^2 \approx 0.95$ ), and simulation confirms the incorrect identification of phase in Figure 14.

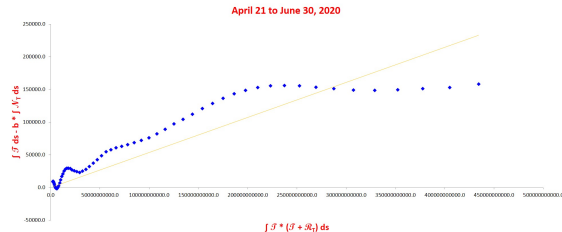


Figure 13: India Phase Plot

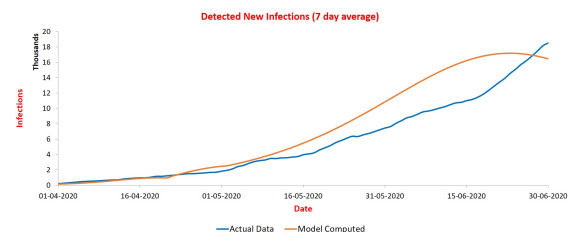


Figure 14: India Trajectory

Removing last ten points results in a better fit (Figure 15) with  $\tilde{\beta} \approx 0.16$ ,  $\frac{1}{\tilde{\rho}} \approx 977.9$ ,  $R^2 \approx 0.99$ ,

and a good simulation (Figure 16).

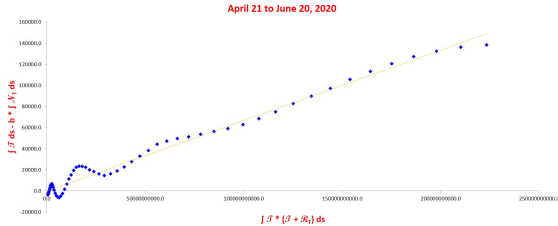


Figure 15: India Phase Plot

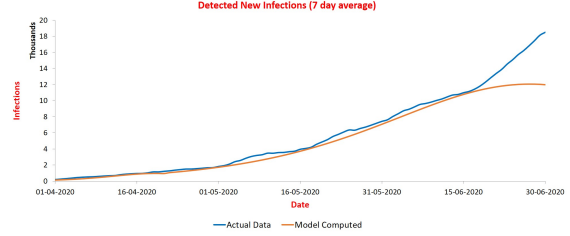


Figure 16: India Trajectory

It can be improved further by ignoring the initial few days as drift period and using the remaining points for estimating the values of parameters. Removing first five days (Figure 17) gives  $\tilde{\beta} \approx 0.16$ ,  $\frac{1}{\tilde{\rho}} \approx 970.6$ ,  $R^2 \approx 0.99$ , and a better simulation (Figure 18). In the plot, points in drift period are colored red. Note that the points oscillate around the line initially which is likely due to errors in reported data.

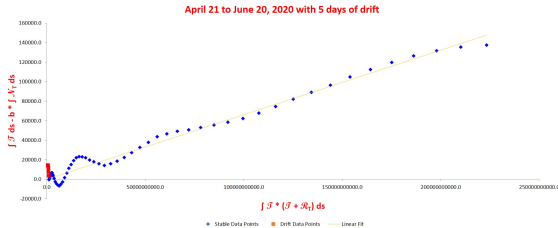


Figure 17: India Phase Plot

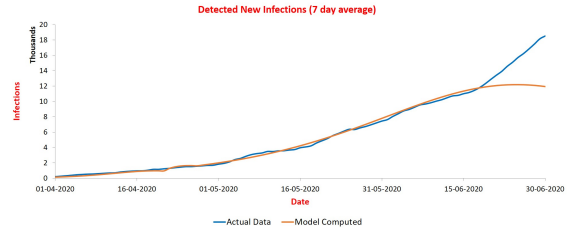


Figure 18: India Trajectory

Above two examples were for the situation when all data points in a phase are available, which implies that the prediction of trajectory is for the past. What about the future? We can predict the future as long as the current phase continues. The parameter estimation for the current phase will not be as precise as for past phases since full phase data is not available. In fact, if the current phase is in drift period, parameter estimation can be significantly off. However, one can detect if the phase is in drift period or stable period by observing the point plot  $\mathcal{P}(t)$  for the current phase, which allows one to infer if the prediction is accurate or not.

For example, trajectory for India was in the drift phase during the first half of April. This caused the model estimation to be significantly off: in a tweet on 14th April [22], we predicted a peak at around 190K infections during April 20-25. The phase plot shows a clear drift (Figure 19) with  $\tilde{\beta} \approx 0.35$  and  $\frac{1}{\tilde{\rho}} \approx 56.8$ . It stabilized by 23rd April leading to much better prediction by 29th April as mentioned in first section. The stability is clearly visible in the phase plot (Figure 20). The estimated parameter values are  $\tilde{\beta} \approx 0.32$  and  $\frac{1}{\tilde{\rho}} \approx 43.2$ .

While addition of next fifteen data points made the predictions more accurate, the projection using only six data points of stable period was already reasonably accurate.

### 7.3 Parameter values during drift period

The above calculations give us values of parameters  $\tilde{\beta}$  and  $\tilde{\rho}$  post the drift period of every phase. However, in order to simulate the course of the pandemic, it is necessary to have the values of the

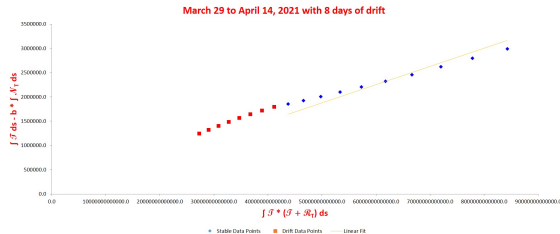


Figure 19: India Phase Plot

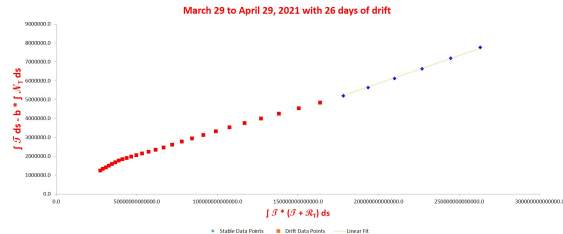


Figure 20: India Phase Plot

parameters during the drift period as well.

Suppose  $d$  is the number of days in drift period, and  $b_0$  and  $b_1$  are the computed values of a parameter in the previous and the current phases. Then its value will move from  $b_0$  to  $b_1$  during the drift period. A natural way of fixing its value during the period is to use either arithmetic or geometric progression. That is, on  $i$ th day in the drift period the value is set to  $b_0 + \frac{i}{d} \cdot (b_1 - b_0)$  or  $b_0 \cdot (\frac{b_1}{b_0})^{i/d}$  respectively.

Among these, geometric progression captures the way parameters change better:

- When a new, more infectious, mutant spreads in a population, its infections grow exponentially initially. This corresponds to a multiplicative increase in  $\beta$ .
- Similarly, a new virus spreads in a region exponentially at the beginning. This corresponds to a multiplicative increase in  $\rho$ .
- A lockdown typically restricts movement sharply causing a multiplicative decrease in  $\beta$ .
- A change in testing strategy typically gets implemented fast in a region, causing a multiplicative change in  $\epsilon$ .

For these reasons, we assume that changes in parameters  $\beta$ ,  $\rho$ , and  $\epsilon$  are multiplicative. Further, terms  $1 - \epsilon$  and  $1 - c$  do not change much during drift period since, as has been observed in actual simulations, both  $\epsilon$  and  $c$  remain close to 0. Therefore, multiplicative changes in  $\epsilon$  and  $c$  almost coincide with multiplicative changes in  $1 - \epsilon$  and  $1 - c$ , and so we can assume that these also change geometrically. This leads to the nice conclusion that changes in  $\tilde{\beta}$  and  $\tilde{\rho}$  are also multiplicative.

## 7.4 Computing Detected Trajectory

Once we have duration, drift periods, and parameter values for all phases, the trajectory of the pandemic can be computed easily.

**Lemma 5.** *Given  $\mathcal{T}(0)$ ,  $\mathcal{R}_T(0)$ ,  $\gamma$ ,  $P_0$ ,  $D_i$ ,  $d_i$ ,  $\tilde{\beta}_i$ , and  $\tilde{\rho}_i$  for  $1 \leq i \leq k$ , where*

- $P_0$  is population of the region,
- $D_i$  and  $d_i$  are respectively duration and drift period of  $i$ th phase,
- $\tilde{\beta}_i$  and  $\tilde{\rho}_i$  are respectively estimated values of parameters for  $i$ th phase,

*the trajectory of detected cases can be computed for the period  $\sum_{i=1}^k D_i$ .*

*Proof.* Proof is by induction on  $t$ . Base case of  $t = 0$  is given as input. Suppose  $\mathcal{T}(t)$ , and  $\mathcal{R}_T(t)$  are computed. Then, from (14):

$$\mathcal{N}_T(t+1) = \tilde{\beta}_t \mathcal{T}(t) - \frac{\tilde{\beta}_t}{\tilde{\rho}_t P_0} (\mathcal{T}(t) + \mathcal{R}_T(t)) \mathcal{T}(t).$$

And

$$\begin{aligned} \mathcal{R}_T(t+1) &= \mathcal{R}_T(t) + \gamma T(t) \\ \mathcal{T}(t+1) &= \mathcal{T}(t) + \mathcal{R}_T(t) + \mathcal{N}_T(t+1) - \mathcal{R}_T(t+1). \end{aligned}$$

where  $\tilde{\beta}_t$  and  $\tilde{\rho}_t$  are values of parameters on day  $t$ .  $\square$

Detected trajectory thus is captured by the  $(4k+4)$ -tuple

$$\mathbb{D} = (\mathcal{T}(0), \mathcal{R}_T(0), P_0, \gamma, D_1, d_1, \tilde{\beta}_1, \tilde{\rho}_1, \dots, D_k, d_k, \tilde{\beta}_k, \tilde{\rho}_k).$$

This shows that detected trajectory can be specified much more compactly than via  $\sum_{i=1}^k D_i$  points  $\mathcal{N}_T(t)$ .

## 8 Actual Trajectory of Pandemic

Similar to quantities associated with detected trajectory, define  $\mathcal{U} = \rho P_0 U$ ,  $\mathcal{M} = \mathcal{U} + \mathcal{T}$ ,  $\mathcal{R} = \rho P_0 R$ , and  $\mathcal{N} = \rho P_0 N$ . The actual trajectory of the pandemic is given by the daily values of  $\mathcal{N}(t)$ . There is no way to measure it directly. Is it possible to compute this trajectory given a detected trajectory? It appears unlikely since detected trajectory only provides  $\tilde{\beta}$  and  $\tilde{\rho}$  values while actual trajectory is determined by four parameter  $\beta$ ,  $\rho$ ,  $\epsilon$  and  $c$ . Given  $\tilde{\beta}$  and  $\tilde{\rho}$ , one needs two more parameters  $\epsilon$  and  $c$  for each phase to compute the entire trajectory:

**Lemma 6.** *Given a detected trajectory  $\mathbb{D}$ , along with  $\mathcal{M}(0)$ ,  $\mathcal{R}(0)$ ,  $\epsilon_i$ , and  $c_i$  for  $1 \leq i \leq k$ , where  $\epsilon_i$  and  $c_i$  are respectively values of parameters  $\epsilon$  and  $c$  for  $i$ th phase, the trajectory of actual cases can be computed for the period  $\sum_{i=1}^k D_i$ .*

*Proof.* Proof is by induction on  $t$ . Base case of  $t = 0$  is given as input. Suppose  $\mathcal{M}(t)$ , and  $\mathcal{R}(t)$  are computed. Then, from SUTRA equations:

$$\begin{aligned} \beta_t &= \frac{\tilde{\beta}_t}{(1 - \epsilon_t)(1 - c_t)} \\ \rho_t &= \frac{\tilde{\rho}_t}{\epsilon_t(1 - c_t)} \\ \mathcal{N}(t+1) &= \beta_t(1 - \epsilon_t) \left( 1 - \frac{1}{\rho_t P_0} (\mathcal{M}(t) + \mathcal{R}(t)) \right) \mathcal{M}(t). \end{aligned}$$

And

$$\begin{aligned} \mathcal{R}(t+1) &= \mathcal{R}(t) + \gamma \mathcal{M}(t) \\ \mathcal{M}(t+1) &= \mathcal{M}(t) + \mathcal{R}(t) + \mathcal{N}(t+1) - \mathcal{R}(t+1). \end{aligned}$$

where  $\tilde{\beta}_t$ ,  $\tilde{\rho}_t$ ,  $\epsilon_t$  and  $c_t$  are values of parameters on day  $t$ .  $\square$

Potentially, there may be infinitely many different actual trajectories for a given detected trajectory. We now prove that, given a detected trajectory and initial values  $\mathcal{M}(0)$  and  $\mathcal{R}(0)$ , there are only *finitely many* actual trajectories. Further, we give a canonical way to identify a *unique trajectory* from them and show how to compute it.

**Theorem 1.** *Given a detected trajectory*

$$\mathbb{D} = (\mathcal{T}(0), \mathcal{R}_T(0), P_0, \gamma, D_1, d_1, \tilde{\beta}_1, \tilde{\rho}_1, \dots, D_k, d_k, \tilde{\beta}_k, \tilde{\rho}_k)$$

along with  $\mathcal{M}(0)$  and  $\mathcal{R}(0)$ , there exist at most  $2^{4\sum_{j=1}^k d_j}$  actual trajectories satisfying the SUTRA model that agree with the given detected trajectory and initial values.

*Proof.* Proof is by induction on the number of phases. In the base case we have only one phase. For this phase,  $d_1 = 0$  since there are no previous values of parameters. Therefore, parameter values stay the same throughout the phase duration of  $D_1$  days. Let  $\beta_1, \rho_1, \epsilon_1$  and  $c_1$  be the parameters governing the actual trajectory for this phase. From equations (9) and (11):

$$\begin{bmatrix} \mathcal{M}(0) \\ \mathcal{R}(0) \end{bmatrix} \approx \begin{bmatrix} \mathcal{T}(0) & 0 \\ \mathcal{R}_T(0) & P_0 \end{bmatrix} \cdot \begin{bmatrix} \frac{1}{\epsilon_1} \\ c_1 \rho_1 \end{bmatrix}$$

giving us excellent approximations of  $\epsilon_1$  and  $c_1 \rho_1$ . From this, we can compute

$$\begin{aligned} \rho_1 &= \tilde{\rho}_1 / \epsilon_1 + \rho_1 c_1 \\ c_1 &= c_1 r_1 / r_1 \\ \beta_1 &= \tilde{\beta}_1 / (1 - \epsilon_1) (1 - c_1) \end{aligned}$$

giving values of all parameters for first phase, using which the trajectory can be computed for the first phase uniquely.

Suppose there are at most  $2^{2\sum_{j=1}^{i-1} d_j}$  trajectories up to phase  $i - 1$ . Fix any one trajectory with values of four parameters in phase  $i - 1$  being  $\beta_{i-1}, \rho_{i-1}, \epsilon_{i-1}$  and  $c_{i-1}$ . Let  $t_0 = \sum_{j=1}^{i-1} D_j$ . We have:

$$\begin{bmatrix} \mathcal{M}(t_0) \\ \mathcal{R}(t_0) \end{bmatrix} = \frac{1}{\epsilon_{i-1}} \begin{bmatrix} \mathcal{T}(t_0) \\ \mathcal{R}_T(t_0) \end{bmatrix} + c_{i-1} \rho_{i-1} \begin{bmatrix} 0 \\ P_0 \end{bmatrix}.$$

Phase  $i$  has a drift period of  $d_i$  days and, as we have argued, the parameter values change multiplicatively during the period. Let  $\epsilon_{i,j} = \epsilon_{i-1} x^j$ , and  $1 - c_{i,j} = (1 - c_{i-1}) / y^j$  for  $1 \leq j \leq d_i$ , where  $x$  and  $y$  are unknown multipliers by which the two parameters change every day. The final value of the parameters will be  $\epsilon_i = \epsilon_{i-1} x^{d_i}$  and  $1 - c_i = (1 - c_{i-1}) / y^{d_i}$ .

Let  $\tilde{\beta}_{i,j} = \tilde{\beta}_{i-1} (\frac{\tilde{\beta}_i}{\tilde{\beta}_{i-1}})^{j/d_i}$  and  $\tilde{\rho}_{i,j} = \tilde{\rho}_{i-1} (\frac{\tilde{\rho}_i}{\tilde{\rho}_{i-1}})^{j/d_i}$ , for  $1 \leq j \leq d_i$ . These numbers can be computed since  $\tilde{\beta}_{i-1}, \tilde{\beta}_i, \tilde{\rho}_{i-1}$ , and  $\tilde{\rho}_i$  are known.

Let  $\beta_{i,j} = \frac{\tilde{\beta}_{i,j}}{(1 - \epsilon_{i,j})(1 - c_{i,j})}$  and  $\rho_{i,j} = \frac{\tilde{\rho}_{i,j}}{\epsilon_{i,j}(1 - c_{i,j})}$  for  $1 \leq j \leq d_i$ . Then we can write:

$$\begin{bmatrix} \mathcal{M}(t_0 + j) \\ \mathcal{R}(t_0 + j) \end{bmatrix} = \begin{bmatrix} g_j & 0 \\ \gamma & 1 \end{bmatrix} \cdot \begin{bmatrix} \mathcal{M}(t_0 + j - 1) \\ \mathcal{R}(t_0 + j - 1) \end{bmatrix}$$

where

$$\begin{aligned}
g_j &= \beta_{i,j-1}(1 - \epsilon_{i,j-1})(1 - \frac{\mathcal{M}(t_0 + j - 1) + \mathcal{R}(t_0 + j - 1)}{\rho_{i,j-1} P_0}) - \gamma + 1 \\
&= \tilde{\beta}_{i,j-1}(\frac{1}{1 - c_{i,j-1}} - \frac{\epsilon_{i,j-1}}{\tilde{\rho}_{i,j-1}} \frac{\mathcal{M}(t_0 + j - 1) + \mathcal{R}(t_0 + j - 1)}{P_0}) - \gamma + 1 \\
&= \tilde{\beta}_{i,j-1}(\frac{y^{j-1}}{1 - c_{i-1}} - \frac{\epsilon_{i-1} x^{j-1}}{\tilde{\rho}_{i,j-1}} \frac{\mathcal{M}(t_0 + j - 1) + \mathcal{R}(t_0 + j - 1)}{P_0}) - \gamma + 1
\end{aligned}$$

Therefore, both  $\mathcal{M}(t_0 + j)$  and  $\mathcal{R}(t_0 + j)$  are polynomials in  $x$  and  $y$ . It is straightforward to show that the degrees of  $\mathcal{M}(t_0 + j)$  and  $\mathcal{R}(t_0 + j)$  equal  $2^j - j - 1$  and  $2^{j-1} - j - 2$  respectively.

At the end of drift period, we have:

$$\begin{aligned}
\begin{bmatrix} \mathcal{M}(t_0 + d_i) \\ \mathcal{R}(t_0 + d_i) \end{bmatrix} &= \frac{1}{\epsilon_i} \begin{bmatrix} \mathcal{T}(t_0 + d_i) \\ \mathcal{R}_T(t_0 + d_i) \end{bmatrix} + c_i \rho_i \begin{bmatrix} 0 \\ P_0 \end{bmatrix} \\
&= \frac{1}{\epsilon_i} \begin{bmatrix} \mathcal{T}(t_0 + d_i) \\ \mathcal{R}_T(t_0 + d_i) \end{bmatrix} + c_i \frac{\tilde{\rho}_i}{\epsilon_i(1 - c_i)} \begin{bmatrix} 0 \\ P_0 \end{bmatrix} \\
&= \frac{1}{\epsilon_{i-1} x^{d_i}} \begin{bmatrix} \mathcal{T}(t_0 + d_i) \\ \mathcal{R}_T(t_0 + d_i) \end{bmatrix} + \frac{\tilde{\rho}_i}{\epsilon_{i-1} x^{d_i}} (\frac{y^{d_i}}{1 - c_{i-1}} - 1) \begin{bmatrix} 0 \\ P_0 \end{bmatrix}
\end{aligned} \tag{18}$$

For  $t_0 + d_i < t \leq t_0 + D_i$ , it inductively follows that:

$$\begin{aligned}
\begin{bmatrix} \mathcal{M}(t) \\ \mathcal{R}(t) \end{bmatrix} &= \begin{bmatrix} \beta_i(1 - \epsilon_i)S(t-1) - \gamma + 1 & 0 \\ \gamma & 1 \end{bmatrix} \cdot \begin{bmatrix} \mathcal{M}(t-1) \\ \mathcal{R}(t-1) \end{bmatrix} \\
&= \begin{bmatrix} \beta_i(1 - \epsilon_i)S(t-1) - \gamma + 1 & 0 \\ \gamma & 1 \end{bmatrix} \cdot \left( \frac{1}{\epsilon_i} \begin{bmatrix} \mathcal{T}(t-1) \\ \mathcal{R}_T(t-1) \end{bmatrix} + c_i \rho_i \begin{bmatrix} 0 \\ P_0 \end{bmatrix} \right) \\
&= \frac{1}{\epsilon_i} \begin{bmatrix} \mathcal{T}(t) \\ \mathcal{R}_T(t) \end{bmatrix} + c_i \rho_i \begin{bmatrix} 0 \\ P_0 \end{bmatrix}
\end{aligned} \tag{19}$$

Therefore, once the relationship is satisfied between actual and detected cases after drift period, it remains valid for rest of the phase.

For what values of unknown multipliers  $x$  and  $y$  is the relationship satisfied? Equation (18) provides two polynomials in  $x$  and  $y$ :

$$\begin{bmatrix} Q_M(x, y) \\ Q_R(x, y) \end{bmatrix} = x^{d_i} \begin{bmatrix} \mathcal{M}(t_0 + d_i) \\ \mathcal{R}(t_0 + d_i) \end{bmatrix} - \frac{1}{\epsilon_{i-1}} \begin{bmatrix} \mathcal{T}(t_0 + d_i) \\ \mathcal{R}_T(t_0 + d_i) \end{bmatrix} - \frac{\tilde{\rho}_i}{\epsilon_{i-1}} (\frac{y^{d_i}}{1 - c_{i-1}} - 1) \begin{bmatrix} 0 \\ P_0 \end{bmatrix}.$$

with  $Q_M(x, y)$  of degree  $2^{d_i} - 1$  and  $Q_R(x, y)$  of degree  $2^{d_i-1} - 2$ , such that the actual multipliers are their common roots. Lemma 7 shows that the number of common roots of these two polynomials that correspond to a valid solution is at most  $2^{4d_i}$ . Therefore, the number of possible trajectories after  $i$  phases is bounded by  $2^{2 \sum_{j=1}^i d_j}$ .  $\square$

**Lemma 7.** *Number of common roots of polynomials  $Q_M(x, y)$  and  $Q_R(x, y)$  that correspond to a valid solution is at most  $2^{4d_i}$ .*

Although the upper bound on the number of trajectories is quite large, in practice, most of the common roots of the polynomials  $Q_M$  and  $Q_R$  would not satisfy one or more of following conditions that should be true for any actual trajectory:

$$0 < \beta < 1, \quad 0 < \epsilon < 1, \quad 0 < \rho < 2, \quad -1 < c < 1.$$

Therefore, most can be eliminated. Further, the value of parameter  $\epsilon$  is unlikely to change significantly from one phase to next since testing strategies do not change dramatically in a short period. This leads to following definition: Given an actual trajectory up to phase  $i - 1$ , its *canonical extension* to phase  $i$  is the actual trajectory for phase  $i$  such that  $|\epsilon_i - \epsilon_{i-1}|$  is minimum. The *canonical* actual trajectory is the trajectory obtained by taking the unique trajectory of phase 1 and canonically extending it for subsequent phases.

In practice, we have observed that for most of the phases, there is only one actual trajectory corresponding to the computed detected trajectory that satisfies the abovementioned range for parameters, which then becomes the canonical actual trajectory.

## 8.1 Computing Canonical Trajectory

Given canonical trajectory up to phase  $i - 1$ , its canonical extension for phase  $i$  can be computed using standard gradient descent method for each phase provided there is no error in data. However, if data has errors, polynomials  $Q_M$  and  $Q_R$  may not have any common root that corresponds to a feasible trajectory. In such a situation, which is almost always true in practice, we use the method used in proof of Lemma 7.

Observe that when data has errors, even the relationships of equation (19) will not hold. Define polynomials:

$$\begin{aligned} Q_{M,t}(x, y) &= x^{d_i}(\mathcal{M}(t) + \mathcal{R}(t)) - \frac{1}{\epsilon_{i-1}}(\mathcal{T}(t) + \mathcal{R}_T(t) + \frac{\tilde{\beta}_i P_0}{1 - c_{i-1}} y^{d_i} - \tilde{\beta}_i P_0) \\ Q_{R,t}(x, y) &= x^{d_i}(\mathcal{R}(t)) - \frac{1}{\epsilon_{i-1}}(\mathcal{R}_T(t) + \frac{\tilde{\beta}_i P_0}{1 - c_{i-1}} y^{d_i} - \tilde{\beta}_i P_0) \end{aligned}$$

And combine them as:

$$P(x, y) = Q_M^2(x, y) + Q_R^2(x, y) + \sum_{t=t_0+d_i+1}^{t_0+D_i} (Q_{M,t}^2(x, y) + Q_{R,t}^2(x, y)).$$

Instead of finding zeroes of all the polynomials, we find minima of  $P$ . Since  $\epsilon_i$  is likely to be close to  $\epsilon_{i-1}$  and the same would be true for  $1 - c_i$  and  $1 - c_{i-1}$ , we choose  $(x, y) = (1, 1)$  as the starting point. This results in following algorithm:

1. Let  $P_x = \frac{\partial P}{\partial x}$  and  $P_y = \frac{\partial P}{\partial y}$ ;
2. Find a common root of polynomials  $P_x$  and  $P_y$  using Newton's gradient descent method, starting from point  $(1, 1)$ ;

Note that the common root in the above algorithm can be found quickly even though the degree of polynomials  $P_x$  and  $P_y$  is exponential, since evaluation of the polynomials and their partial derivatives on any point can be done efficiently.

The above algorithm computes canonical trajectory for all phase except the first one. The trajectory of the first phase cannot be computed since  $\mathcal{M}(0)$  and  $\mathcal{R}(0)$  values are not known and therefore, neither are  $\epsilon_1$  and  $c_1$ . We can estimate  $c_1$  by observing that at time  $t = 0$ , the pandemic is in its initial stages and so  $R(0) \approx 0$ . This, in turn implies that  $\frac{1}{\epsilon_1} R_T(0) \approx 0$  and so  $c_1 \approx 0$ .

This only leaves  $\epsilon_1$  as unknown. We can get a good estimate of  $\epsilon_1$  if a serosurvey of the region under consideration is done at any point of time, say at  $t_s$ . The survey provides an estimate of

$\mathcal{R}(t_s)$ . Varying  $\epsilon_1$ , we can compute different canonical trajectories and find the one for which the trajectory-computed value of  $\mathcal{R}(t_s)$  comes close to the serosurvey result. We call this step *calibrating the model*. More than one serosurveys allow fine-tuning of  $\epsilon_1$ , and thus better calibration.

The above analysis leads to the following corollary of Theorem 1:

**Corollary 1.** *For a detected trajectory  $\mathbb{D}$ , its canonical actual trajectory is given by  $\mathbb{A} = (\epsilon_1, \mathbb{D})$ .*

## 8.2 Error Estimates for Parameters

Error estimates for all the parameters can be derived using the estimates for  $\tilde{\beta}$  and  $\tilde{\rho}$  in the following way: use upper and lower bounds of parameters  $\tilde{\beta}$  and  $\tilde{\rho}$  (for their 95% CI values) in the polynomial  $P(x, y)$  and compute the values  $\epsilon$  and  $c$  that minimize  $P$ . These provide upper and lower bounds for  $\epsilon$  and  $c$  respectively. Using these, compute upper and lower bounds for other two parameters  $\beta$  and  $\rho$ . Thus we get 95% CI range of values for all the parameters.

## 9 SUTRA and SIR Trajectories

Both detected and actual trajectories of SUTRA model are a concatenation of multiple SIR trajectories, one for each phase.

**Theorem 2.** *For stable period of phase  $i$ :*

- *Detected trajectory is the trajectory of an SIR model with contact parameter  $\tilde{\beta}_i$  and population  $\tilde{\rho}_i P_0$ .*
- *Actual trajectory is the trajectory of an SIR model with contact parameter  $\beta_i(1 - \epsilon_i)$  and population  $\rho_i P_0$ .*

*Proof.* We have

$$\begin{aligned} \frac{\dot{S}}{1 - c_i} &= -\beta_i \frac{S}{1 - c_i} U = -\frac{\beta_i(1 - \epsilon_i)}{\epsilon_i} \frac{S}{1 - c_i} T = -\tilde{\beta}_i \frac{S}{1 - c_i} \frac{\mathcal{T}}{\tilde{\rho}_i P_0} \\ \frac{\dot{\mathcal{T}}}{\tilde{\rho}_i P_0} &= \frac{1}{\epsilon_i(1 - c_i)} \dot{T} = \frac{1}{\epsilon_i(1 - c_i)} (\beta_i(1 - \epsilon_i) ST - \gamma T) = \tilde{\beta}_i \frac{S}{1 - c_i} \frac{\mathcal{T}}{\tilde{\rho}_i P_0} - \gamma \frac{\mathcal{T}}{\tilde{\rho}_i P_0} \\ \frac{\dot{\mathcal{R}}_T}{\tilde{\rho}_i P_0} &= \frac{1}{\epsilon_i(1 - c_i)} \dot{R}_T = \frac{1}{\epsilon_i(1 - c_i)} \gamma T = \gamma \frac{\mathcal{T}}{\tilde{\rho}_i P_0} \end{aligned}$$

Therefore,  $\hat{S} = \frac{S}{1 - c_i}$ ,  $\hat{T} = \frac{\mathcal{T}}{\tilde{\rho}_i P_0}$ , and  $\hat{R}_T = \frac{\mathcal{R}_T}{\tilde{\rho}_i P_0}$  follow SIR trajectory with contact rate  $\tilde{\beta}_i$ , removal rate  $\gamma$ , and population  $\tilde{\rho}_i P_0$ .

For the actual trajectory, we have

$$\begin{aligned} \dot{S} &= -\beta_i S U = \beta_i(1 - \epsilon_i) S M = -\beta_i(1 - \epsilon_i) S \frac{\mathcal{M}}{\rho_i P_0} \\ \frac{\dot{\mathcal{M}}}{\rho_i P_0} &= \beta_i(1 - \epsilon_i) S \frac{\mathcal{M}}{\epsilon_i P_0} - \gamma \frac{\mathcal{M}}{\rho_i P_0} \\ \frac{\dot{\mathcal{R}}}{\rho_i P_0} &= \gamma \frac{\mathcal{M}}{\rho_i P_0} \end{aligned}$$

Therefore,  $S$ ,  $M = \frac{\mathcal{M}}{\rho_i P_0}$ , and  $R = \frac{\mathcal{R}}{\rho_i P_0}$  follow SIR trajectory with contact rate  $\beta_i(1 - \epsilon_i)$ , removal rate  $\gamma$ , and population  $\rho_i P_0$ .  $\square$

During the drift period of a phase, SUTRA trajectory transitions from one SIR trajectory to another. The above theorem explains why Covid-19 trajectories for short periods could be captured well by SIR models or their variants. The theorem also allows us to estimate the peak of active infections, both for detected and actual trajectories.

### 9.1 Peak of Active Infections

If active infections in detected trajectory peak in phase  $i$ ,  $\hat{S} = \frac{\gamma}{\beta_i}$  at the peak. Since

$$\begin{aligned}\hat{S} &= 1 - (\hat{M} + \hat{R}) \\ &= 1 - \frac{\mathcal{T} + \mathcal{R}_T}{\tilde{\rho}_i P_0}\end{aligned}$$

the condition is equivalent to:

$$\mathcal{T} + \mathcal{R}_T = \tilde{\rho}_i P_0 \left(1 - \frac{\gamma}{\tilde{\beta}_i}\right).$$

Active infections in actual trajectory will also peak at roughly the same time: if peak is during stable phase, then  $\mathcal{M} = \frac{1}{\epsilon_i} \mathcal{T}$  and so the peak of  $\mathcal{M}$  is on the same day as peak of  $\mathcal{T}$ ; and if peak occurs during drift period, the peak of  $\mathcal{M}$  may differ slightly. The peak occurs at  $S = (1 - c_i) \frac{\gamma}{\beta_i} = \frac{\gamma}{\beta_i(1 - \epsilon_i)}$ , and therefore, *basic reproduction number*  $R_0 = \frac{\beta_i(1 - \epsilon_i)}{\gamma}$ .

Since the SUTRA trajectory is a concatenation of multiple SIR trajectories with different parameter values, the trajectory may have multiple peaks. A phase will have a peak whenever cumulative reported infections cross  $\tilde{\rho} P_0 (1 - \frac{\gamma}{\tilde{\beta}})$  in the phase with  $\tilde{\rho}$  and  $\tilde{\beta}$  being parameter values for the phase.

## 10 Loss of Immunity and Vaccination Induced Immunity

It is well-established that some infected people lose immunity over time [7]. This causes a transition from  $R$  back to  $S$ . On the other hand, vaccination of a person in  $S$  can directly move him or her to  $R$  without going through  $U$  or  $T$  groups. As the time progresses, number of both types of cases rise and start impacting the dynamics of the pandemic. In this section, we show that the revised dynamics is easily captured in SUTRA.

Immunity loss and vaccination cause movement between groups  $S$  and  $R$ . Let  $L_U(t)$  and  $L_T(t)$  be the fraction of people that move at time  $t$  from  $S$  to  $R_U$  and to  $R_T$  respectively. Note that  $L_U(t)$  would be negative if people move from  $R_U$  to  $S$  and similarly for  $R_T$ . The equations governing the dynamics change as follows:

$$\begin{aligned}\dot{S} &= -\beta S U - L_U - L_T \\ \dot{U} &= \beta S U - \epsilon \beta S U - \gamma U \\ \dot{T} &= \epsilon \beta S U - \gamma T \\ \dot{R}_U &= \gamma U + L_U \\ \dot{R}_T &= \gamma T + L_T\end{aligned}$$

We have:

$$\dot{M} + \gamma M = \frac{1}{\epsilon} (\dot{T} + \gamma T)$$

leading to the relationship (as shown in section 4)

$$M = \frac{1}{\epsilon}T + de^{-\gamma t}.$$

Therefore, as argued earlier, we can still assume  $M = \frac{1}{\epsilon}T$  after the drift period of every phase.

Define  $R_{0,U}$  and  $R_{0,T}$  as:

$$\begin{aligned}\dot{R}_{0,U} &= \gamma U, R_{0,U}(0) = R_U(0) \\ \dot{R}_{0,T} &= \gamma T, R_{0,T}(0) = R_T(0)\end{aligned}$$

Let  $\rho P_0$  be the effective population at time  $t$ , and  $\mathcal{R}_0(t) = \rho P_0(R_{0,U}(t) + R_{0,T}(t))$  as usual. Let  $\mathcal{L}(t)$  be the cumulative number of cases that transition from  $S$  to  $R$  via immunity loss or vaccination until time  $t$ . Then:

**Lemma 8.**  $\mathcal{R}(t) = \mathcal{R}_0(t) + \mathcal{L}(t)$ .

*Proof.* Follows immediately from the observation that  $\dot{R} - \dot{R}_0 = L_U + L_T$ .  $\square$

Let  $N(t)$  be the fraction of population infected at time  $t$  as usual. The following lemma is crucial:

**Lemma 9.**

$$N = \beta(1 - \epsilon)(1 - \frac{\mathcal{L}}{\rho P_0})(1 - \frac{\mathcal{M} + \mathcal{R}_0}{\rho(1 - \frac{\mathcal{L}}{\rho P_0})P_0})M.$$

*Proof.* We have:

$$\begin{aligned}N &= \beta S U \\ &= \beta(1 - \epsilon) S M \\ &= \beta(1 - \epsilon)(1 - (M + R))M \\ &= \beta(1 - \epsilon)(1 - \frac{\mathcal{M} + \mathcal{R}_0 + \mathcal{L}}{\rho P_0})M \\ &= \beta(1 - \epsilon)(1 - \frac{\mathcal{L}}{\rho P_0} - \frac{\mathcal{M} + \mathcal{R}_0}{\rho P_0})M \\ &= \beta(1 - \epsilon)(1 - \frac{\mathcal{L}}{\rho P_0})(1 - \frac{\mathcal{M} + \mathcal{R}_0}{\rho(1 - \frac{\mathcal{L}}{\rho P_0})P_0})M.\end{aligned}$$

$\square$

The above lemma shows that:

**Corollary 2.** *The trajectory  $N(t)$  of the modified model equals the SUTRA trajectory with both  $\beta$  and  $\rho$  multiplied by  $1 - \frac{\mathcal{L}}{\rho P_0}$ .*

Therefore, ones does not need to modify the model in order to capture the effect of immunity loss and vaccination on the trajectory. The computed detected trajectory from the reported data  $N_T(t)$  provides the values  $\tilde{\beta} = \beta(1 - \epsilon)(1 - c)(1 - \frac{\mathcal{L}}{\rho P_0})$  and  $\tilde{\rho} = \epsilon \rho(1 - c)(1 - \frac{\mathcal{L}}{\rho P_0})$  incorporating their impact and thus the model still captures the detected trajectory well. Computing actual trajectory from these parameter values provides values  $\beta(1 - \frac{\mathcal{L}}{\rho P_0})$ ,  $\rho(1 - \frac{\mathcal{L}}{\rho P_0})$ ,  $\epsilon$  and  $c$  for every phase. While this means that we do not get the real values of  $\beta$  and  $\rho$  unless  $\mathcal{L}$  is estimated, we can use the computed values to predict the near future well.

A byproduct of adjustment in parameter  $\tilde{\rho}$  is that it may decrease over time: this will happen when change in  $\mathcal{L}$  is positive during the drift period of a phase. This is best viewed as reduction in effective population due to vaccination.

## 11 Application of SUTRA Model

Simulations for multiple countries, large number of states and districts of India show that the relationship in equation (15) between detected quantities holds universally. As a consequence, SUTRA model is able to match the pandemic trajectory in these regions quite well (simulation for India, its states and districts are available at [32]). This suggests that the pandemic dynamics are close to the dynamics of SUTRA model. In this section, we discuss applications of the model.

### 11.1 Predicting Short-Term Future

Given the detected pandemic trajectory up to time  $t$  for a region, we can estimate the parameter values of phases until time  $t$ . If the last phase has entered stable period then the trajectory of the pandemic can be predicted reasonably well for time beyond  $t$  as long as parameters do not change substantially. A couple of examples of this are already provided in first section, and in section 7.2.3, it is shown how the predictions changed when the phase stabilized for India in April this year.

An interesting aspect of the prediction for India made on 14th April [22] is that while the peak value was way off the mark, the predicted timing of the peak was not too far from actual one. Also, the estimate of  $\tilde{\beta}$  was reasonably close, but not the estimate of  $\tilde{\rho}$  suggesting that reach was changing significantly in the period. Both the observations are connected. If  $\tilde{\beta}$  is approximated well, then the timing of the predicted peak will also be well approximated.

**Lemma 10.** *Let  $\mathbb{D} = (\mathcal{T}(t_0), \mathcal{R}_T(t_0), P_0, \gamma, D, d, \tilde{\beta}, \tilde{\rho})$  be the phase of a detected trajectory starting at time  $t_0$  with drift period of  $d$  and total duration of  $D$  such that the trajectory peaks during the phase. Let  $\mathbb{A}$  be the phase of actual trajectory corresponding to  $\mathbb{D}$  with parameters  $\beta$ ,  $\rho$ ,  $\epsilon$ , and  $c$ . Then detected trajectory  $\mathbb{D}' = (\mathcal{T}(t_0), \mathcal{R}_T(t_0), P_0, \gamma, D, d, \tilde{\beta}, \tilde{\rho}')$  peaks close to  $\mathbb{D}$  for  $\tilde{\rho}' \neq \tilde{\rho}$  provided  $\epsilon, c, \frac{\tilde{\rho}'}{\tilde{\rho}}\epsilon \ll 1$ .*

*Proof.* Consider the actual trajectory with same initial conditions as  $\mathbb{A}$  and with parameters  $\rho$  and  $\beta' = \tilde{\beta}/(1 - \epsilon')(1 - c)$  where  $\epsilon' = \tilde{\rho}'/\rho(1 - c) = \frac{\tilde{\rho}'}{\rho}\epsilon$ . Since  $\epsilon, \epsilon' \ll 1$ ,  $1 - \epsilon' \approx 1 - \epsilon$  which implies that  $\beta \approx \beta'$ . Therefore, trajectories  $\mathbb{A}$  and  $\mathbb{A}'$  move close to each other and so their peaks will also be close.

Consider a detected trajectory obtained from  $\mathbb{A}'$  that detects  $\epsilon'$  fraction of cases after the drift period. There will be a unique  $c'$  that will satisfy the required conditions for this trajectory. Since  $c \ll 1$  and  $1 - \epsilon \approx 1 - \epsilon'$ ,  $1 - c \approx 1 - c'$ . And therefore,  $\tilde{\beta}'' = \beta'(1 - \epsilon')(1 - c') \approx \tilde{\beta}$  and  $\tilde{\rho}'' = \epsilon'\rho(1 - c') \approx \tilde{\rho}'$ . This implies that the resulting detected trajectory  $\mathbb{D}'' = (\mathcal{T}(t_0), \mathcal{R}_T(t_0), P_0, \gamma, D, d, \tilde{\beta}'', \tilde{\rho}'')$  is close to  $\mathbb{D}'$ . We now have the following sequence of connections: peak date of  $\mathbb{D}$  is same as that of  $\mathbb{A}$ , which is close to peak date of  $\mathbb{A}'$ , which is same as peak date of  $\mathbb{D}''$ , which is close to peak date of  $\mathbb{D}'$ .  $\square$

Typically  $\epsilon, c, \frac{\tilde{\rho}'}{\tilde{\rho}}\epsilon \ll 1$ , and so the conclusions of lemma would generally be applicable.

### 11.2 Predicting Long-Term Future

In the long-term, the current values of parameters are very likely to change, and so in order to predict the trajectory well into the future, one needs to guess future values of parameters. This is not possible. However, one can aim to create different possible trajectories of the pandemic by estimating parameter values under reasonable assumptions. Let us see how:

- The value of  $\beta$  depends on the infectivity of virus and behavior of people. One can consider various scenarios for this: one is to assume that society resumes normal life with the current virus remaining active. Another is to assume that society resumes normal life and a new mutant arrives that is significantly more infectious than the current variant.
- The value of  $\rho$  can be 1 at maximum, and eventually it attains that value. So one can assume  $\rho = 1$  for future scenarios.
- The value of  $\epsilon$  seems to remain almost stationary for the entire duration of pandemic and the same can be assumed for future.
- If  $\epsilon$  does not change, neither will  $c$ .
- Effect of loss of immunity and vaccination can be incorporated by estimating the multiplier to  $\beta$  and  $\rho$  as per Corollary 2. One would need to estimate the fraction of population that loses immunity and fraction that gains immunity due to vaccination for future time periods.

Suppose

$$\mathbb{D} = (\mathcal{T}(0), \mathcal{R}_T(0), P_0, \gamma, D_1, d_1, \tilde{\beta}_1, \tilde{\rho}_1, \dots, D_k, d_k, \tilde{\beta}_k, \tilde{\rho}_k)$$

is the detected trajectory until now. To compute trajectory for a future scenario, we do the following:

- Pick a suitable number of days, say  $D$ , for which prediction is to be done and a drift period  $d$  for the phase.
- Estimate the value of  $\mathcal{L}$  until now and add  $\ell$  to it in the next  $D$  days.
- Compute  $\rho = \rho_k + \frac{\mathcal{L}}{P_0}$ , where  $\rho_k$  is the reach at present. Then  $\rho$  is the real reach at present.
- Set  $\tilde{\beta}_{k+1} = m \frac{1-(\mathcal{L}+\ell)/P_0}{1-\mathcal{L}/(\rho P_0)} \tilde{\beta}_k$ , where  $m$  is the multiplier chosen based on estimation of people movement and dominant mutant.
- Set  $\tilde{\rho}_{k+1} = \frac{1-(\mathcal{L}+\ell)/P_0}{\rho_k} \tilde{\rho}_k$ .
- Compute the trajectory

$$\mathbb{D}_F = (\mathbb{D}, D, d, \tilde{\beta}_{k+1}, \tilde{\rho}_{k+1})$$

Note that in order to compute  $\tilde{\beta}_{k+1}$  and  $\tilde{\rho}_{k+1}$ , knowledge of  $\rho_k$  is required, which is possible only if the model can be calibrated to compute the actual trajectory.

### 11.3 Understanding the Past

Given the detected pandemic trajectory up to time  $t$  for a region, we can compute number of phases and parameter values  $\tilde{\beta}$  and  $\tilde{\rho}$  for each. If we have one serosurvey result for the region, the model can be calibrated and values of all parameters can be computed. Each phase change denotes a significant change in one or more parameter values. This can occur due to expansion of pandemic's reach, or spread of a more infectious mutant, or administrative actions. The parameter values provide a quantification of the impact of such events. We do this analysis for India and US.

### 11.3.1 India Analysis

Table 1 provides phases, their duration, and values of all parameters (within 95% CI), for India until now. Calibration of the model was done using two serosurveys: [27] and [14]. The value of  $1/\epsilon_1$  obtained through calibration is marked in red color. Figure 21 shows the plot of detected trajectory, both the actual and model-computed.

Table 1: Parameter Table for India

Phase	Start	Drift	$\beta$	$1/\epsilon$	$100\rho$
1	02 Mar	5	$0.32 \pm 0.03$	33	$0 \pm 0$
2	20 Mar	0	$0.26 \pm 0.01$	$33 \pm 0$	$0.1 \pm 0$
3	24 Apr	5	$0.16 \pm 0.01$	$33 \pm 0$	$3.6 \pm 0.3$
4	21 Jun	30	$0.16 \pm 0$	$33 \pm 0$	$20 \pm 1.4$
5	22 Aug	10	$0.15 \pm 0$	$33 \pm 0$	$40.3 \pm 1.1$
6	02 Nov	10	$0.2 \pm 0.04$	$33 \pm 0$	$39.5 \pm 5.3$
7	01 Jan	10	$0.23 \pm 0.01$	$33 \pm 0$	$39.7 \pm 0.9$
8	10 Feb	40	$0.38 \pm 0.01$	$33 \pm 0$	$48.3 \pm 1.2$
9	29 Mar	26	$0.28 \pm 0.01$	$33 \pm 0$	$85.3 \pm 1.8$
10	25 May	3	$0.28 \pm 0.06$	$33 \pm 0$	$87.3 \pm 5.6$
11	18 Jun	42	$0.5 \pm 0.04$	$33 \pm 0$	$95.1 \pm 1.5$
12	23 Aug	2	$0.65 \pm 0.21$	$33 \pm 0$	$93.4 \pm 4.5$

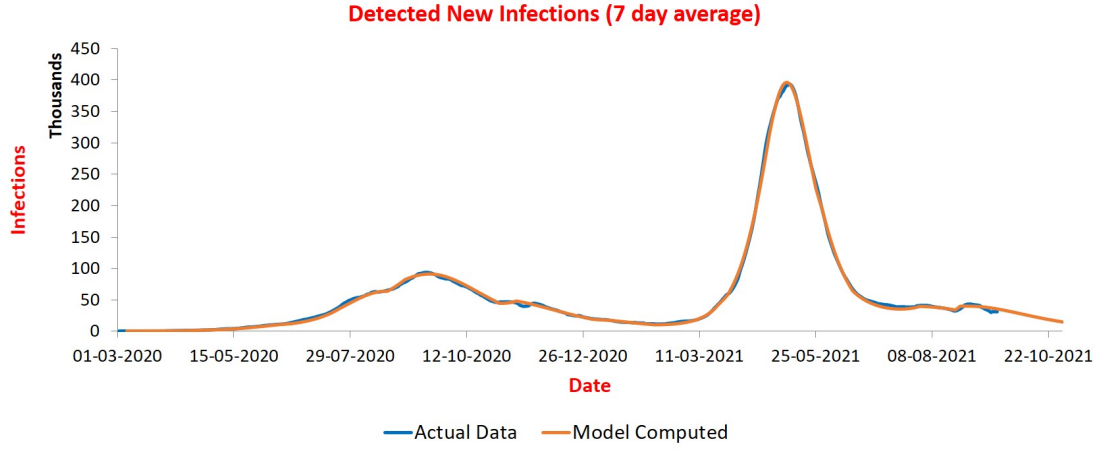


Figure 21: Detected Trajectory for India

The parameter values provide a good understanding of the pandemic progression in the country. A strict lockdown was imposed in March-end 2020. Value of parameter  $\beta$  before the lockdown was 0.32. It came down to 0.16 soon after the lockdown and remained at the same level until October-end. Value of  $\rho$  stayed very small until middle of June due to severe restrictions on movement. A reverse migration of workers started in May and continued until June-end. Many of these migrants took the virus to different parts of the country, resulting in a sharp increase

in  $\rho$  from June-mid (time lag is because migrants took a while to reach their destination). The value of  $\rho$  stabilized at around 0.4 in August-end. Increase from July was also influenced by successive relaxations in lockdown. The first wave peaked in mid-September when  $\mathcal{T} + \mathcal{R}_T$  crossed  $\tilde{\rho}P_0(1 - \frac{\gamma}{\beta}) \approx \rho\epsilon P_0(1 - \frac{1}{10\beta}) \approx \frac{0.4}{33} \cdot \frac{1}{3}P_0 \approx 5.5$  million. Removal of restrictions from November caused  $\beta$  to increase to 0.24 by January.

The second wave started in March this year caused by a significant increase in value of  $\beta$  to  $\approx 0.38$ . This increase was due to more infectious  $\delta$ -variant as well as people becoming careless. While the variant was still spreading to different regions of the country, several states imposed lockdowns in April causing  $\beta$  to come down to 0.28. In March and April, reach more than doubled to  $\approx 0.85$ . Coupled with relatively high value of  $\beta$ , it caused a significantly higher peak this time in May when  $\mathcal{T} + \mathcal{R}_T$  crossed  $\tilde{\rho}P_0(1 - \frac{\gamma}{\beta}) \approx \rho\epsilon P_0(1 - \frac{1}{10\beta}) \approx \frac{0.85}{33} \cdot \frac{9}{14}P_0 \approx 22.7$  million. With lockdowns significantly removed and spread of  $\delta$ -variant to the whole country, the value of  $\beta$  has climbed up to 0.65 at present (although the 95% CI range is quite wide). This rise in  $\beta$  caused another small peak in early-September when  $\mathcal{T} + \mathcal{R}_R$  crossed  $\tilde{\rho}P_0(1 - \frac{\gamma}{\beta}) \approx \rho\epsilon P_0(1 - \frac{1}{10\beta}) \approx \frac{0.93}{33} \cdot \frac{11}{13}P_0 \approx 32.8$  million. The peak was barely visible since infected population was already above 75% by then.

At present, reach is close to maximum possible (although  $\rho \approx 93\%$ , actual value of reach is likely to be higher due to vaccination factor) and infected population is  $\sim 80\%$ .

### 11.3.2 USA Analysis

Table 2 provides phases, their duration, and values of all parameters (within 95% CI), for US until now. Calibration of the model was done using [5] that records that until May 2021, one in 4.2 cases were detected. The value of  $1/\epsilon_1$  obtained through calibration is marked in red color. 22 shows the plot of detected trajectory, both the actual and model-computed.

Table 2: Parameter Table for US

Ph No	Start	Drift	$\beta$	$1/\epsilon$	$100\rho$
1	15-03-2020	3	$0.32 \pm 0.02$	4	$0.8 \pm 0.1$
2	13-04-2020	32	$0.15 \pm 0$	$4 \pm 0$	$5.1 \pm 0.1$
3	11-06-2020	10	$0.17 \pm 0.01$	$4.1 \pm 0.1$	$13.7 \pm 1.1$
4	13-09-2020	45	$0.23 \pm 0.01$	$4.2 \pm 0.1$	$29.3 \pm 1$
5	01-12-2020	10	$0.23 \pm 0.02$	$4.2 \pm 0$	$39.3 \pm 2.6$
6	30-12-2020	5	$0.27 \pm 0.02$	$4.2 \pm 0$	$45.9 \pm 1.3$
7	19-02-2021	7	$0.23 \pm 0.02$	$4.2 \pm 0$	$54.9 \pm 2.5$
8	08-03-2021	16	$0.52 \pm 0.06$	$4.4 \pm 0.2$	$50.9 \pm 3.1$
9	06-06-2021	10	$0.36 \pm 0.02$	$4.4 \pm 0$	$56.8 \pm 0.9$
10	26-06-2021	18	$0.49 \pm 0.02$	$4.5 \pm 0$	$70.5 \pm 1.6$
11	11-08-2021	3	$0.42 \pm 0.04$	$4.8 \pm 0.2$	$77.5 \pm 4$

Value of  $\beta$  started from 0.32 in US as well. With restrictions imposed, it came down significantly and stayed in the range 0.15-0.17 until August. Reach too did not increase much and was limited to around 14% by then. There was a minor peak in July-end due to jump in reach from  $\sim 5\%$  to  $\sim 14\%$ . Parameter  $\beta$  then increased a bit and stayed in the range 0.23-0.27 for the next six months. In the same period, reach increased continuously to around 55%. This increase was responsible

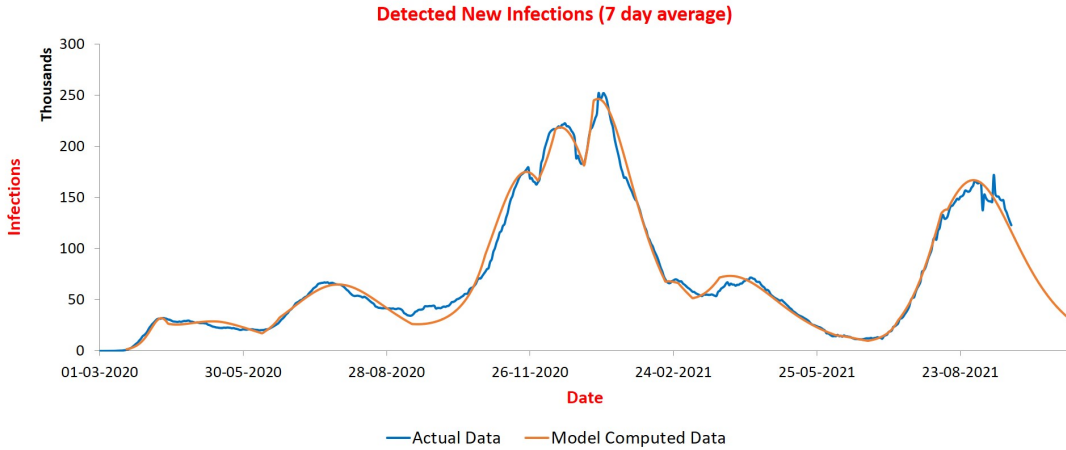


Figure 22: Detected Trajectory for US

for the three jagged, increasingly higher peaks during November to January since increase in  $\rho$  by factor  $m$  pushes the cumulative infection ( $= \mathcal{T} + \mathcal{R}_T$ ) value for peak higher by the same factor.

A sharp rise in  $\beta$  in March suggests that  $\delta$ -variant may have spread by April. The following phase 9 shows substantial drop in value of  $\beta$  but only for a short period. By middle of July it went back up to  $\sim 0.5$  and reach increased substantially too. This caused the latest peak in early-September.

Value of  $\rho$  at present is around 77% of population. Of course, as Corollary 2 shows, there is an unknown multiplier to it due to vaccination and loss of immunity and therefore, the actual reach may be higher. Percentage of infected population at present is  $\sim 60\%$ .

## 12 Conclusions and Future Work

The results presented here demonstrate conclusively that the SUTRA model is quite capable of predicting the course of the COVID-19 pandemic across a variety of countries, and a variety of situations. A similar approach could be applied to other communicable diseases as well.

The SUTRA model has enough flexibility to adopt to different situations easily, as demonstrated in incorporating effects of vaccination and immunity loss. There is one weakness in the model: when it is in drift period of a phase, prediction of future trajectory becomes difficult. It would be worthwhile to investigate if eventual values of parameters can be predicted by observing the drift pattern. This will help improve the predictions of the model.

## Acknowledgements

The work of MA and MV was supported by the Science and Engineering Research Board, India.

## References

[1] R.M. Anderson and R.M. May. *Infectious Diseases of Humans: Dynamics and Control*. Oxford University Press, 1991.

[2] Santosh Ansumali, Shaurya Kaushal, AlokeKumar, Meher K. Prakash, and M.Vidyasagar. Modelling a pandemic with asymptomatic patients, impact of lockdown and herd immunity, with applications to SARS-CoV-2. *Annual Reviews in Control*, 50:432–447, 2020.

[3] F. Brauer, P. van den Driessche, and J. Wu (Eds.). *Mathematical Epidemiology*. Springer, 2008.

[4] Byrne AW, McEvoy D, Collins AB, et al. Inferred duration of infectious period of SARS-CoV-2: rapid scoping review and analysis of available evidence for asymptomatic and symptomatic COVID-19 cases. *BMJ Open*, 10, 2020.

[5] CDC, USA. Estimated COVID-19 Burden. <https://www.cdc.gov/coronavirus/2019-ncov/cases-updates/burden.html>, July 2021.

[6] USA Center for Disease Control, Atlanta. <https://www.cdc.gov/flu/pandemic-resources/1918-pandemic-h1n1.html>, 2021.

[7] Christian Holm Hansen, Daniela Michlmayr, Sophie Madeleine Gubbels et al. Assessment of protection against reinfection with SARS-CoV-2 among 4 million PCR-tested individuals in Denmark in 2020: a population-level observational study. *The Lancet*, 397, 2021.

[8] Daniel Owusu, Mary A Pomeroy, Nathaniel M Lewis et al. Persistent SARS-CoV-2 RNA Shedding Without Evidence of Infectiousness: A Cohort Study of Individuals With COVID-19. *The Journal of Infectious Diseases*, 2021.

[9] O. Diekmann and J. A. P. Heesterbeek. *Mathematical epidemiology of infectious diseases*. Wiley, 2000.

[10] Klaus Dietz. Transmission and control of arbovirus diseases. In D. Ludwig and K. L. Cooke, editors, *Epidemiology*, pages 104–121. Society for Industrial and Applied Mathematics (SIAM), 1975.

[11] Paul Fine, Ken Eames, and David L. Heymann. “herd immunity”: A rough guide. *Clinical Infectious Diseases*, 52(7):911–916, 2011.

[12] G. Calafiore, C. Novara and C. Possieri. A time-varying SIRD model for the Covid-19 contagion in Italy. *Annual Reviews in Control*, 2020.

[13] Giordano, G., Blanchini, F., Bruno, R. et al. Modelling the COVID-19 epidemic and implementation of population-wide interventions in Italy. *Nature Medicine*, 26:855–860, 2020.

[14] ICMR Surveillance Group. <http://loksabhaph.nic.in/Questions/QResult15.aspx?qref=24949&lsno=17>, July 2021.

[15] Herbert W. Hethcote. The mathematics of infectious diseases. *SIAM Review*, 42(4):399–453, 2000.

[16] Mark Honigsbaum. Revisiting the 1957 and 1968 influenza pandemics. *The Lancet*, 395(10240):1824–1826, 13 June 2020.

[17] Indian SARS-COV-2 Genomics Sequencing Consortium. Sequencing in India. <https://dbtindia.gov.in/insacog>, 2021.

[18] M. Keeling and P. Rohani. *Modelling Infectious Diseases in Humans and Animals*. Princeton University Press, 2008.

[19] William Ogilvy Kermack and A. G. McKendrick. A contribution to the mathematical theory of epidemics. *Proceedings of The Royal Society A*, 117(772):700–721, 1927.

[20] Michael Y. Li and James S. Muldowney. Global stability for the SEIR model in epidemiology. *Mathematical Biology*, 125:155–164, 1995.

[21] Wei-Min Liu, Herbert W. Hethcote, and Simon A. Levin. Dynamical behavior of epidemiological models with nonlinear incidence rates. *Journal of Mathematical Biology*, 25:359–380, 1987.

[22] Manindra Agrawal. Tweet on 14th April. <https://twitter.com/agrawalmanindra/status/1382264866874880002?s=21> April 2021.

[23] Manindra Agrawal. Tweet on 25th July. <https://twitter.com/agrawalmanindra/status/1419176814954500096?s=21> July 2021.

[24] Manindra Agrawal. Tweet on 29th April. <https://twitter.com/agrawalmanindra/status/1387734516807073792?s=21> April 2021.

[25] M. Martcheva. *An introduction to mathematical epidemiology*, volume 61. Springer, 2015.

[26] Michael Debabrata Patra, Jibin Jose, Kunal Priyadarshi et al. State of the Economy. [https://rbidocs.rbi.org.in/rdocs/Bulletin/PDFs/01AR\\_15072021F163007EFACA4764BCD6FAF0D3E0ADB3.PDF](https://rbidocs.rbi.org.in/rdocs/Bulletin/PDFs/01AR_15072021F163007EFACA4764BCD6FAF0D3E0ADB3.PDF) July 2021.

[27] Murhekar MV, Bhatnagar T, and Thangaraj JWV et al. SARS-CoV-2 seroprevalence among the general population and healthcare workers in India. *Int J Infect Dis.*, July 2021.

[28] Narendra Kumar, Shafeeq K. Shahul Hameed, Giridhara R. Babu et al. Descriptive epidemiology of SARS-CoV-2 infection in Karnataka state, South India: Transmission dynamics of symptomatic vs. asymptomatic infections. *EClinicalMedicine*, 2021.

[29] Huffington Post. Threat Of COVID-19 Third Wave Ruins Europe's Christmas Vacation. [https://www.huffpost.com/entry/europe-christmas-plans-covid-19-third-wave\\_n\\_5fda235ac5b62f31c202320b](https://www.huffpost.com/entry/europe-christmas-plans-covid-19-third-wave_n_5fda235ac5b62f31c202320b), Accessed December 25 2020.

[30] Marguerite Robinson and Nikolaos I. Stilianakis. A model for the emergence of drug resistance in the presence of asymptomatic infections. *Mathematical Biosciences*, 243(2):163–177, 2013.

[31] C. E. G. Smith. Prospects for the control of infectious disease. *Proceedings of the Royal Society of Medicine*, 63:1181–1190, 1970.

[32] SUTRA Consortium. SUTRA Predictions for India. <https://www.sutra-india.in>, September 2021.

[33] W.W.C. Topley and G. S. Wilson. The spread of bacterial infection: the problem of herd immunity. *Journal of Hygiene*, 21:243–249, 1923.

[34] Worldometers. COVID-19 Coronavirus Pandemic. <https://www.worldometers.info/coronavirus/>, 24 September 2021.

## Appendix

We prove:

**Lemma 7.** *Number of common roots of polynomials  $Q_M(x, y)$  and  $Q_R(x, y)$  that correspond to a valid solution is at most  $2^{4d_i}$ .*

*Proof.* A valid solution of the equations  $Q_M(x, y) = 0 = Q_R(x, y)$  needs to be tolerant of errors in reported data  $\mathcal{N}_T(t)$ : one should get a neighboring point as solution if there are small errors in data. We capture this property by introducing error in  $\mathcal{N}_T(t_0)$ . Write

$$\begin{aligned} \begin{bmatrix} Q_M(x, y) \\ Q_R(x, y) \end{bmatrix} &= x^{d_i} G \cdot \begin{bmatrix} \mathcal{M}(t_0) \\ \mathcal{R}(t_0) \end{bmatrix} - \frac{1}{\epsilon_{i-1}} \begin{bmatrix} \mathcal{T}(t_0 + d_i) \\ \mathcal{R}_T(t_0 + d_i) \end{bmatrix} - \frac{\tilde{\rho}_i}{\epsilon_{i-1}} \left( \frac{y^{d_i}}{1 - c_{i-1}} - 1 \right) \begin{bmatrix} 0 \\ P_0 \end{bmatrix} \\ &= \frac{x^{d_i}}{\epsilon_{i-1}} G \cdot \begin{bmatrix} \mathcal{T}(t_0) \\ \mathcal{R}_T(t_0) \end{bmatrix} + x^{d_i} c_{i-1} \rho_{i-1} G \cdot \begin{bmatrix} 0 \\ P_0 \end{bmatrix} \\ &\quad - \frac{1}{\epsilon_{i-1}} \begin{bmatrix} \mathcal{T}(t_0 + d_i) \\ \mathcal{R}_T(t_0 + d_i) \end{bmatrix} - \frac{\tilde{\rho}_i}{\epsilon_{i-1}} \left( \frac{y^{d_i}}{1 - c_{i-1}} - 1 \right) \begin{bmatrix} 0 \\ P_0 \end{bmatrix} \end{aligned}$$

where

$$G = \prod_{j=1}^i \begin{bmatrix} g_j & 0 \\ \gamma & 1 \end{bmatrix} = \begin{bmatrix} g & 0 \\ h & 1 \end{bmatrix}.$$

Define polynomials

$$\begin{aligned} \begin{bmatrix} P_M(x, y, \xi) \\ P_R(x, y, \xi) \end{bmatrix} &= \frac{x^{d_i}}{\epsilon_{i-1}} G \cdot \begin{bmatrix} \mathcal{T}(t_0) + \xi \\ \mathcal{R}_T(t_0) \end{bmatrix} + x^{d_i} c_{i-1} \rho_{i-1} G \cdot \begin{bmatrix} 0 \\ P_0 \end{bmatrix} \\ &\quad - \frac{1}{\epsilon_{i-1}} \begin{bmatrix} \mathcal{T}(t_0 + d_i) \\ \mathcal{R}_T(t_0 + d_i) \end{bmatrix} - \frac{\tilde{\rho}_i}{\epsilon_{i-1}} \left( \frac{y^{d_i}}{1 - c_{i-1}} - 1 \right) \begin{bmatrix} 0 \\ P_0 \end{bmatrix} \end{aligned}$$

where  $\xi$  is error in reporting of  $\mathcal{N}_T(t_0)$ . We have:

$$\begin{bmatrix} P_M(x, y, \xi) \\ P_R(x, y, \xi) \end{bmatrix} = \begin{bmatrix} Q_M(x, y) \\ Q_R(x, y) \end{bmatrix} + \frac{x^{d_i} \xi}{\epsilon_{i-1}} \begin{bmatrix} g \\ h \end{bmatrix}.$$

Let

$$P(x, y, \xi) = P_M^2(x, y, \xi) + P_R^2(x, y, \xi)$$

and fix error  $\xi$  to an arbitrary small value. Then a point  $(x_0, y_0)$  that corresponds to a valid solution of  $Q_M(x, y) = 0 = Q_R(x, y)$  will have a neighboring point  $(x_1, y_1)$  on which  $P$  is minimized. In other words,  $(x_1, y_1)$  is a solution of  $\frac{\partial P}{\partial x} = 0 = \frac{\partial P}{\partial y}$ . For  $\nu_k \in \mathbb{R}$ ,  $|\nu_k|$  close to zero, suppose  $\frac{\partial P(x, y, \nu_k)}{\partial x}$  and  $\frac{\partial P(x, y, \nu_k)}{\partial y}$  have a common irreducible factor say  $f_k \in \mathbb{R}[x, y]$ . Then  $\frac{\partial P}{\partial x}, \frac{\partial P}{\partial y} \in (f_k, \xi - \nu_k) = I_k$ , a prime ideal in  $\mathbb{R}[x, y, \xi]$ . Ideals  $I_k$  and  $I_{k'}$  are comaximal for  $k \neq k'$  and therefore, their intersection is same as product ideal. Therefore,  $\frac{\partial P}{\partial x}$  and  $\frac{\partial P}{\partial y}$  are not in intersection of more than finitely many  $I_k$ 's. Fix a  $\nu_k$ ,  $|\nu_k|$  close to zero, for which  $\frac{\partial P(x, y, \nu_k)}{\partial x}$  and  $\frac{\partial P(x, y, \nu_k)}{\partial y}$  do not have a common factor. By Bezout's Theorem, the number of common solutions of  $\frac{\partial P(x, y, \nu_k)}{\partial x} = 0 = \frac{\partial P(x, y, \nu_k)}{\partial y}$  are then bounded by the product of their degrees which is less than  $2^{4d_i}$ . For small enough  $\nu_k$ , each solution of  $Q_M(x, y) = 0 = Q_R(x, y)$  would correspond to exactly one solution of  $\frac{\partial P(x, y, \nu_k)}{\partial x} = 0 = \frac{\partial P(x, y, \nu_k)}{\partial y}$ . Therefore, the number of valid solutions of  $Q_M(x, y) = 0 = Q_R(x, y)$  is bounded by  $2^{4d_i}$ .  $\square$